PALEOCEANOGRAPHY, VOL. 15, NO. 6, PAGES 642-658 DECEMBER 2000

Similar glacial and interglacial export bioproductivity in the Atlantic sector of the Southern Ocean: Multiproxy evidence and implications for glacial atmospheric CO_2

Martin Frank,[1,2] Rainer Gersonde,[3] Michiel Rutgers van der Loeff,[3] Gerhard Bohrmann,[4] Christine C. Nürnberg,[4] Peter W. Kubik,[5] Martin Suter,[6] and Augusto Mangini[1]

Abstract. We present time series of export productivity proxy data including $^{230}Th_{ex}$-normalized deposition rates (rain rates) of ^{10}Be, dissolution-corrected biogenic Ba, and biogenic opal as well as authigenic U concentrations which are complemented by rain rates of total (detrital) Fe and sea ice indicating diatom abundances from five sediment cores across the Atlantic sector of the Southern Ocean covering the past 150,000 years. The results suggest that ^{10}Be rain rates and authigenic U concentration cannot serve as quantitative paleoproductivity proxies because they have also been influenced by detrital particle fluxes in the case of ^{10}Be and bulk sedimentation rates (sediment focussing) and deep water oxygenation in the case of U.The combined results of the remaining productivity proxies of this study (rain rates of biogenic opal and biogenic Ba in those sections without authigenic U) and other previously published proxy data from the Southern Ocean ($^{231}Pa/^{230}Th$ and nitrogen isotopes) suggest that a combination of sea ice cover, shallow remineralization depth, and stratification of the glacial water column south of the present position of the Antarctic Polar Front and possibly Fe fertilization north of it have been the main controlling factors of export paleoproductivity in the Southern Ocean over the last 150,000 years. An overall glacial increase of export paleoproductivity is not supported by the data, implying that bioproductivity variations in the Southern Ocean are unlikely to have contributed to the major glacial atmospheric CO_2 drawdown observed in ice cores.

1. Introduction

Enhanced export bioproductivity caused by a more efficient utilization of available nutrients in the high-nutrient low-chlorophyll (HNLC) surface waters of the Southern Ocean was invoked by modelers to have contributed to lowering glacial atmospheric CO_2 concentrations [*Knox and McElroy*, 1984; *Siegenthaler and Wenk*, 1984; *Sarmiento and Toggweiler*, 1984] recorded in ice cores [cf. *Barnola et al.*, 1987].

Increased productivity is expected to result in a reduced nutrient concentration of the surface waters. The major proxy for surface water nutrient concentrations is the stable carbon isotope ratio ($\delta^{13}C$) of planktonic foraminifera. However, neither last glacial Southern Ocean $\delta^{13}C$ records obtained from planktonic foraminifera [*Labeyrie and Duplessy*, 1985; *Charles and Fairbanks*, 1990] nor those obtained from organic matter [*Shemesh et al.*, 1993; *Singer and Shemesh*, 1995] show evidence for decreased nutrient concentrations but show a shift which rather indicates an increase. Comparison of glacial and interglacial biogenic opal accumulation rates in sediments from the Atlantic sector of the Southern Ocean showed a 5° glacial northward shift of the area of high opal accumulation but apparently did not support a scenario of increased glacial productivity because of similar overall glacial and interglacial accumulation rates [*Charles et al.*, 1991; *Mortlock et al.*, 1991], which were, however, not corrected for sediment redistribution effects.

The above nutrient-based models to explain lowered glacial atmospheric CO_2 concentrations regained attention by the finding that the availability of dissolved Fe is biolimiting in the HNLC surface waters of the equatorial Pacific and the Southern Ocean [*Martin et al.*, 1994; *deBaar et al.*, 1995; *Coale et al.*, 1996; *Behrenfeld et al.*, 1996]. Iron fertilization leading to increased glacial export productivity was also concluded from an innovative study using Late Quaternary trace element ($^{231}Pa_{ex}/^{230}Th_{ex}$, $^{10}Be/^{230}Th_{ex}$, and authigenic U) deposition in sediments from the eastern Atlantic sector of the Southern Ocean as paleo tracers for biogenic particle flux [*Kumar et al.*, 1995]. These new proxies are supposed to be independent of the strong and often variable sediment redistribution intensity caused by bottom currents which can severely bias conventional reconstructions of sedimentary fluxes from Southern Ocean sediments, and they are also not affected by variable preservation efficiency of biogenic compounds. Higher glacial than interglacial dust fluxes originating from Patagonia [*De Angelis et al.*, 1987; *Petit et al.*, 1990; *Grousset et al.*, 1992], which partly dissolved and released Fe to the surface waters, were invoked as the mechanism which lifted Fe limitation in Southern Ocean surface waters and permitted increased export productivity

[1]Heidelberger Akademie der Wissenschaften, Institut für Umweltphysik, Universität Heidelberg, Heidelberg, Germany.
[2]Now at Institute for Isotope Geology and Mineral Resources, Department of Earth Sciences, ETH Zentrum, Zurich, Switzerland.
[3]Alfred-Wegener-Institut für Polar- und Meeresforschung, Bremerhaven, Germany.
[4]GEOMAR, Forschungszentrum für marine Geowissenschaften, Kiel, Germany.
[5]Paul Scherrer Institut, c/o Institut für Teilchenphysik der ETH Zurich, ETH-Hönggerberg, Zurich, Switzerland.
[6]Institut für Teilchenphysik der ETH Zurich, ETH-Hönggerberg, Zurich, Switzerland.

Paper number 2000PA000497.
0883-8305/00/2000PA000497$12.00

[*Martin*, 1990, *Kumar et al.*, 1995; *Moore et al.*, 2000]. However, results of a more recent study which combined records of nitrogen isotopes and proxies for export paleoproductivity (biogenic opal, $^{231}Pa_{ex}/^{230}Th_{ex}$, authigenic U, and biogenic Ba (Ba_{bio})) from sediments in the Atlantic and Indian sectors of the Southern Ocean suggested that overall glacial export productivity may not have been increased and has also, overall, been much lower than in the highly productive upwelling areas at ocean margins [*Francois et al.*, 1997]. Instead, a stratification of the glacial Southern Ocean water column south of the present position of the Antarctic Polar Front (APF), which greatly inhibited the transfer of CO_2 and nutrients to the surface water, was suggested by these authors to have contributed to lowering glacial atmospheric CO_2. Similar results were recently obtained from a modeling study [*Stephens and Keeling*, 2000] and from a new approach to reconstruct surface water nutrient levels [*Elderfield and Rickaby*, 2000], both invoking glacial stratification caused by sea ice cover. Stratification has also recently been suggested to explain the sharp drop of opal productivity after 2.73 Ma in the subarctic North Pacific Ocean [*Haug et al.*, 1999].

In this study we compare the overall glacial and interglacial export productivity in the Southern Ocean, applying a multiproxy approach including deposition rates of ^{10}Be, total (detrital) Fe, biogenic Ba, biogenic opal, and concentrations of authigenic U. Considering that sea ice is one of the prominent environmental factors controlling Southern Ocean export productivity [*Abelmann and Gersonde*, 1991], we combine our data with estimations of past sea ice variations obtained from the occurrence pattern of sea ice indicating diatom abundances. We present these results for five sediment cores on a N-S transect across the Antarctic Circumpolar Current System (ACC) in the eastern Atlantic sector of the Southern Ocean. All cores except one document the past 150 kyr, thus including the last two terminations.

2. Proxies

The Southern Ocean is a highly dynamic hydrographic regime where fluxes of particles supplied laterally by strong bottom currents [*Petschick et al.*, 1996; *Diekmann et al.*, 1999] can exceed the vertical components of the fluxes by up to a factor of 20 [*Francois et al.*, 1993; *Yu*, 1994; *Yu et al.*, 1996; *Kumar et al.*, 1995; *Frank et al.*, 1996, 1999; *Asmus et al.*, 1999]. For any realistic reconstruction of particle fluxes from sediments in the Southern Ocean it is thus essential to correct for these laterally supplied components or the results can not be considered quantitatively reliable [e.g., *Ikehara et al.*, 2000]. The "true" vertical particle fluxes (rain rates) can be reconstructed by normalization of the fluxes of each component to initial $^{230}Th_{ex}$ (ex denotes exceeding the radioactive equilibrium with ^{234}U in the detrital particles), the flux of which is assumed to match its local constant production rate in the water column [*Bacon and Rosholt*, 1982; *Bacon*, 1984, *Francois et al.*, 1990, 1993] within some uncertainties [*Henderson et al.*, 1999; *Frank et al.*, 1999].

Rain rates of the radionuclide ^{10}Be exceed the value expected from its cosmogenic production at ocean margins and areas with highly bioproductive surface waters, a process called boundary scavenging [*Spencer et al.*, 1981; *Anderson et al.*, 1990, 1994; *Lao et al.*, 1992b; *Frank et al.*, 1994]. A near-linear relationship between total particle flux and ^{10}Be rain rate allows its use as a paleoflux proxy that is independent from diagenesis and preservation effects [*Kumar et al.*, 1995]. In areas where most of the sediment particles are of biogenic origin, the ^{10}Be rain rate was suggested as a proxy for export productivity [*Kumar et al.*, 1995; *Anderson et al.*, 1998], although there is debate about selective ^{10}Be adsorption to certain species of particles, such as biogenic opal and aluminosilicates (clay minerals) [*Sharma et al.*, 1987; *Bourlès et al.*, 1989a, 1989b; *Lao et al.*, 1992b, 1993; *Wang et al.*, 1997].

At present, export productivity of the HNLC area of the Southern Ocean is dominated by biogenic opal, mainly diatoms. Although seawater is undersaturated with respect to opal, a large portion of it is buried and preserved in Southern Ocean sediments, aided by high sedimentation rates and sediment focusing. Variable dissolution and preservation efficiency [*Broecker and Peng*, 1982; *Pichon et al.*, 1992; *Leynaert et al.*, 1993; *Nelson et al.*, 1995; *Pondaven et al.*, 2000] and differences in opal to organic carbon (C_{org}) ratios [*Kumar et al.*, 1995; *Anderson et al.*, 1998], however, prevent the use of biogenic opal rain rates as independent quantitative tracer of export productivity.

The rain rates of Ba_{bio} (Ba concentrations exceeding the lithogenic background with an atomic Ba/Al ratio of 0.0067 in the Atlantic sector of the Southern Ocean [*Nürnberg et al.*, 1997]), which are closely related to biogenic particle flux and therefore to C_{org}, were suggested to have the advantage of a higher resistance to dissolution compared to biogenic opal and C_{org} and have been used to estimate export productivity [*Dymond et al.*, 1992; *Shimmield et al.*, 1994; *Francois et al.*, 1995, 1997; *Frank et al.*, 1995; *Nürnberg et al.*, 1997; *Dehairs et al.*, 2000; *Jeandel et al.*, 2000]. The relationship between C_{org} and Ba_{bio} is generally explained by suspended barite, which forms during mesopelagic plankton decomposition in or just below the euphotic zone, most probably as precipitates in the sulphate-saturated microenvironments of decaying organic matter mainly associated with diatom frustules [*Dehairs et al.*, 1980; *Bishop*, 1988]. The use of Ba_{bio} as a quantitative tracer of export paleoproductivity is complicated by variable C_{org}/Ba_{bio} ratios observed in sediment traps [*Dymond and Collier*, 1996; *Francois et al.*, 1995] and variable preservation efficiency of Ba_{bio} [*Kumar et al.*, 1996] as a consequence of the understauration of barite in most of the world's deep waters [*Monnin et al.*, 1999]. Recently, it was proposed that the Ba_{bio} signal may already be biased by diagenesis under mildly reducing conditions [*McManus et al.*, 1999] and that the presence of authigenic U may serve to identify non reliable Ba_{bio} signals [*Francois et al.*, 1997; *McManus et al.*, 1998].

Authigenic U itself, which was shown to accumulate in subsurface sediment sections under reducing conditions which are mainly caused by degradation of organic matter [*Cochran and Krishnaswami*, 1980; *Barnes and Cochran*, 1990; *Klinkhammer and Palmer*, 1991], was also suggested to serve as a proxy for export paleoproductivity [*Kumar et al.*, 1995; *Rosenthal et al.*, 1995a, 1995b; *Anderson et al.*, 1998]. The accumulation of authigenic U does, however, not distinguish between C_{org} supplied from the surface water above and C_{org} supplied laterally, which causes an increased U accumulation in focused sediments [*Kumar*, 1994; *Frank et al.*, 1996, 1999; *Francois et al.*, 1997; *Asmus et al.*, 1999]. In addition, low bottom water oxygen levels

also lead to precipitation of authigenic U [*Anderson*, 1987; *Francois et al.*, 1997]. The accumulation of authigenic U enrichments is a function of the bulk sedimentation rate; that is, if the sedimentation rate is low (few centimeters per kiloyear), most C_{org} is oxidized at the sediment-water interface, and no U gradient can develop in the pore water. However, even if authigenic U had been deposited in slowly accumulating sediments, a deepening redoxcline in the sediment column as a consequence of either diminished supply of C_{org} or an increase in bottom water oxygenation can lead to a burn-down and postdepositional removal of authigenic U [e.g., *Jung et al.*, 1997; *Thomson et al.*, 1995; *Rosenthal et al.*, 1995b; *Mangini et al.*, 2000].

In order to investigate to what extent the occurrence of sea ice has been a controlling factor for the biogenic fluxes to the seafloor the particle flux proxies are compared with estimations of past variations of sea ice occurrence. Sediment trap experiments in the seasonally sea ice-covered zone of the Weddell Sea [*Fischer et al.*, 1988; *Abelmann and Gersonde*, 1991; *Gersonde and Zielinski*, 2000] have demonstrated that during sea ice coverage the export of biogenic material from the surface waters is minimal and would not produce a detectable signal in the sediment record. Thus those regions covered year-round by sea ice would only allow the export of low amounts of biogenic matter produced under the ice or in leads. However, in the Atlantic sector of the Southern Ocean, areas that are covered only seasonally by sea ice, such as the central and eastern Weddell Sea south of the ACC, are characterized by low export of biogenic opal [*Abelmann and Gersonde*, 1991; *Gersonde and Zielinski*, 2000] and low opal fluxes to the seafloor [*Schlüter et al.*, 1998], although available nutrients and light during austral summer open water conditions should not limit biogenic productivity in the surface waters. This may be linked to a seasonal stratification caused by melting of previous winter's sea ice [*Stephens and Keeling*, 2000]. The finding of low opal flux to the seafloor south of the ACC is also reproduced by three-dimensional (3-D) inverse modeling of the biogeochemical cycles in the Southern Ocean [*Usbeck*, 1999; *Usbeck and Schlitzer*, 1999]. This study shows that low opal fluxes to the seafloor coincide with appreciable biogenic opal productivity and imply a rapid dissolution in the water column. Radioisotope and TCO_2 data confirm that in the Weddell Gyre, south of the ACC, remineralization of biogenic particles in the upper portion of the water column is enhanced, leading to a strong reduction of biogenic export below ~500 m [*Rutgers van der Loeff and Hoppema*, 1999]. It thus appears that in the Atlantic sector of the Southern Ocean the biogenic flux to the seafloor is reduced south of the ACC. The reasons for this pattern are not yet well understood and are currently the subject of further studies. As the present latitudinal range of this area of low benthic rain rates approximately coincides with the extension of seasonal sea ice, it may be speculated that during glacial time periods, similar

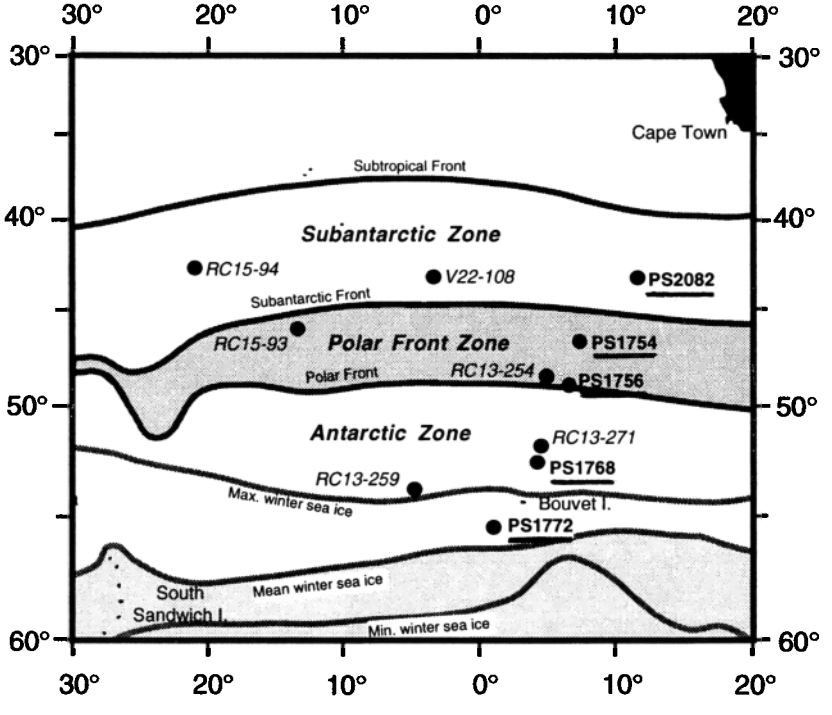

Figure 1. Map of the eastern Atlantic sector of the Southern Ocean showing locations of the cores examined in this study (bold and underlined) and those by *Kumar et al.* [1995] (italics). The present-day average position of the fronts is taken from *Peterson and Stramma* [1991], and the data of the sea ice distribution are from *Fleet Numerical Meteorology and Oceanography Detachment* [1985]. Core descriptions are given by *Frank et al.* [1996]. The Antarctic Zone (AZ) is the area south of the Antarctic Polar Front (APF). The Polar Frontal Zone (PFZ) is located between the APF and the Subantarctic Front (SAF), and the Subantarctic Zone (SAZ) is located north of the SAF. South of the APF, biogenic opal presently dominates the marine sedimentary record (opal belt).

Table 1. Locations of the Cores

Name	Instrument[a]	Location		Water Depth, m	Total Recovery, cm	Sampled Length Presented, cm
		Latitude,°S	Longitude,°E			
PS1772-8	GC	55°27.5'	1°09.8'	4135	1329	400
PS1772-6	MUC	55°27.5'	1°10.0'	4136	24.5	24.5
PS1768-8	GC	52°35.6'	4°28.5'	3270	896	896
PS1768-1	MUC	52°35.5'	4°27.6'	3298	34	34
PS1756-5	GC	48°43.9'	6°42.8'	3787	862	862
PS1756-6	MUC	48°53.7'	6°43.7'	3803	27	27
PS1754-1	GC	46°46.2'	7°36.7'	2471	356	177
PS1754-2	MUC	46°46.0'	7°36.1'	2476	25	25
PS2082-1	GC	43°13.2'	11°44 3'	4610	1391	705
PS2082-3	MUC	43°13.1'	11°45.5'	4661	26	26

[a]GC is gravity core, and MUC is multicore.

conditions controlling biogenic export took place in areas north of 55°S related to the northward expansion of the Antarctic sea ice field.

3. Material and Methods

Five sediment cores (a gravity core complemented by a multicorer for each location to obtain undisturbed sediment surfaces) located on a transect from 43° to 56°S across the eastern Atlantic sector of the ACC (Figure 1) were analyzed in this study. Locations and sample depths are given in Table 1. For cores PS2082-1 [*Mackensen et al.* , 1994], PS1754-1, and PS1768-8 [*Niebler*, 1995], $\delta^{18}O$ stratigraphies are available, whereas the other two cores (PS1772-8 and PS1756-5) do not contain suffcient amounts of foraminifera to produce a reliable $\delta^{18}O$ stratigraphy. A combination of results derived from oxygen isotope stratigraphies (where available), siliceous microfossil biofluctuation stratigraphy, and lithostratigraphy in combination with $^{230}Th_{ex}$ constant flux modeling were used to establish the final stratigraphies for the cores [*Frank et al.*, 1996] (Table 2). The age model used for dating of the marine isotope stages (MIS) follows that of *Martinson et al.* [1987]. Compared with the data published by *Frank et al.* [1996] and *Nürnberg et al.* [1997], the stratigraphy of core PS1756-5 has changed in that MIS boundaries 2/3 (24 ka) and 3/4 (59 ka) [*Martinson et al.*, 1987] had to be readjusted to core depths of 540 cm and 765 cm, respectively, resulting in a total age of only 65 ka for this core. All cores were previously investigated in detail for sediment redistribution processes [*Frank et al.*, 1996, 1999], and the corresponding focusing factors are given in Table 3.

Chemical preparation of the samples for the ^{10}Be accelerator mass spectrometry (AMS) measurements followed closely a previously described method [*Henken-Mellies et al.*, 1990]. The 182 samples of this study were measured at the Zürich AMS facility of the Paul Scherrer Institute and ETH Zürich, Switzerland. They were normalized to the internal standard S555 with a nominal $^{10}Be/^{9}Be$ ratio of 95.5×10^{-12}, and the ^{10}Be rain rates were decay corrected to time of deposition using a half-life of 1.52 Myr [*Hofmann et al.*, 1987]. In order to correctly reconstruct changes of the ^{10}Be rain rates caused by boundary scavenging variations, every ^{10}Be rain rate value was corrected for geomagnetically induced production rate changes of ^{10}Be [*Lao et al.*, 1992a; *Guyodo and Valet*, 1996; *Frank et al.*, 1997]. Because the ^{10}Be data of this study were included in the calculation of a global ^{10}Be stack to reconstruct geomagnetic field intensity variations [*Frank et al.*, 1997], we used the paleointensity reconstruction of *Guyodo and Valet* [1996] to correct for changes in ^{10}Be production rate. This correction is important because of an inferred variability in the production rate of cosmogenic radionuclides of up to 50% above present values during the last 150 kyr [*Bard et al.*, 1990; *Frank et al.*, 1997] and was also applied to the data of *Kumar et al.* [1995] to enable a direct comparison of the data of both studies.

Biogenic opal was determined by X-ray diffraction [*Eisma and van der Gaast*, 1971; *Hempel and Bohrmann*, 1990]. The Ba_{bio} rain rates of all cores except PS1754-1 and the multicores

Table 2. Age Models of the Cores[a]

$\delta^{18}O$-Based MIS	Age, kyr B.P.	Depth, cm				
		PS1772-8	PS1768-8	PS1756-5	PS1754-1	PS2082-1
-	10.06 (^{14}C)	-	54	-	-	-
-	11.26 (^{14}C)	-	78	-	-	-
1	12	17	97	10	22	33
-	14.16 (^{14}C)		142	-	-	-
2	24	55	244	540	54	245
3.13	44	-	-	-	-	300
3	59	80	469	765	78	370
4	74	100	585	-	88	440
5.4	111	136	730	-	140	523
5	130	360	830	-	160	570
6.4	153	-	-	-	-	730
6	190	460	-	-	-	900

[a]Stratigraphy of the cores as derived from the sources referenced to in the text.

Table 3. Focusing Factors[a]

δ^{18}O-Based	Age,	Focusing Factor ψ						
MIS	kyr B.P.	PS1772-8	PS1768-8	PS1756-5	PS1754-1	PS2082-1	PS2498-1	PS2499-5
1	0-12	0.6	4.6[c]	0.8	1.2	2.0[c]	5.7[c]	2.2[c]
2	12-24	2.1[c]	6.0[c]	3.4[c]	0.75	7.7[c]	3.8[c]	7.7[c]
2/3-3.13	24-44	-	-	-	-	1.2		
3.13-3/4	44-59	0.3[b]	3.5[c]	0.7	0.15[b]	2.9[c]	6.3[c]	1.5[c]
4	59-74	0.85	4.6[c]	2.1?[c]	0.5[b]	2.6[c]	3.1[c]	1.8[c]
4/5-5.4	74-111	0.55	1.9[c]	-	0.5[b]	2.3[c]		
5.4-5/6	111-130	0.8	1.6[c]	-	0.5[b]	2.7[c]	5.1[c]	1
5/6-6.4	130-153	-	-	-	-	2.9[c]		
6.4-6/7	153-190	0.9	-	-	-	2.4[c]		

[a]Focusing factor ψ for certain δ^{18}O-based marine isotope stages (MIS) of the five cores presented [*Frank et al.*, 1999] and two additional recently published records [*Asmus et al.* , 1999]. The ages of the MIS boundaries were assigned following *Martinson et al.* [1987].

[b]ψ is significantly smaller than 1 (≤ 0.5); sediment winnowing occurred.

[c]ψ is significantly above 1 (≥ 1.5); sediment focusing occurred.

corresponding to the gravity cores have been published previously [*Nürnberg et al.*, 1997]. The rain rates of Ba_{bio} given in this study are corrected for preservation according to *Dymond et al.* [1992] and *Francois et al.* [1995]. Although water masses south of the APF are saturated with respect to pure barite above 1500-2500 m [*Monnin et al.*, 1999], the above preservation correction has been applied for all cores, including PS1754-1 from 2470 m water depth because it is not clear whether the evidence for barite saturation can be transferred to this location in the Polar Frontal Zone (PFZ) and also because 2500 m is the lower limit where saturation was observed. Concentrations of bulk Fe as well Ba and Al of those samples not given by *Nürnberg et al.* [1997] were determined by atomic absorption spectrometry (AAS) applying standard procedures. Chemical preparation and measurement of ^{238}U and ^{232}Th activities by α spectrometry followed standard procedures [*Frank et al.*, 1994]. Authigenic uranium concentrations were determined by subtracting 23% of the ^{232}Th concentration of each sample from the total ^{238}U concentration, which accounts for the mean detrital Th/U ratio of continental crust [*Wedepohl*, 1995] and which is also reflected in pelagic sediments [*Anderson et al.*, 1998].

The sea ice proxy was established on the basis of a combined study of annual diatom transfer from the Southern Ocean surface to the seafloor using time series sediment traps and mapping of diatom assemblages preserved in surface sediments [*Gersonde and Zielinski*, 2000]. We prefer using this method for the estimation of past sea ice extent and its variations over the approach presented by *Crosta et al.* [1998a, 1998b]. Both methods give approximately the same location of the winter sea ice edge. *Crosta et al.* [1998a] proposed to reconstruct sea ice presence in numbers of months per year based on a statistical method (modern analog technique). This implies that the annual duration of sea ice coverage at a given location is reflected by the production and deposition of diatom sea ice signals. However, such a relationship was disproved by sediment trap experiments documenting that the sea ice signal in the diatom assemblages is produced under austral summer open water conditions from diatom blooms that have been seeded from sea ice to open water [*Gersonde and Zielinski*, 2000]. In addition, the statistical approach may lead to misinterpretations of duration of sea ice coverage in those areas that are affected by enhanced opal dissolution, e.g., in areas with longer annual sea ice coverage. This may lead to the reconstruction of glacial sea ice occurrences that are shorter than during interglacials, as presented by *Crosta et al.* [1998b] from sites located south of the present Polar Front.

In the approach used, relative amounts of the sea ice indicator diatoms *Fragilariopsis cylindrus* and *F. curta* of > 3% of the total assemblages are interpreted as representative for the presence of seasonal winter sea ice in Southern Ocean sediments. Summer sea ice occurrence, which implies permanent or nearly permanent annual sea ice coverage, is signaled by distinct drops in sedimentation rates as a result of strongly reduced or lacking biogenic export and the presence of > 3% of the species *Fragilariopsis obliquecostata*, which is related to water temperatures near freezing point and sea ice formation ($\geq$ - 1.5°C) [*Zielinski and Gersonde*, 1997]. All data are available on request from the corresponding author or electronically at the PANGAEA database, Alfred-Wegener-Institut für Polar- und Meeresforschung, Columbusstrasse, 27568 Bremerhaven, Germany, info@pangaea.de (URL: *www.pangaea.de*).

4. Results

The ^{10}Be rain rates in the five cores (Figure 2a-c) have mostly, in particular during glacials, exceeded the global average production rate [*Monaghan et al.*, 1985/86] by about a factor of 2-3 during the past 150 kyr, which confirms that the Southern Ocean has been a sink for particle reactive trace metals due to its high particle fluxes [*Kumar et al.*, 1995; *Yu et al.*, 1996]. Throughout the transect except the southernmost core PS1772-8, ^{10}Be rain rates show maximum values during the glacial MIS 2-4 (12-59 ka) and 6 (130-190 ka). During MIS 1 (12 ka to present) and 5e (130-111 ka), ^{10}Be rain rates were at minimum, partly even slightly below the global average production rate, indicating an export of ^{10}Be from these locations to areas of higher particle fluxes. These patterns of the ^{10}Be rain rates show a very good correlation with rain rates of Fe and Al_2O_3 (record not displayed), whether located north or south of the APF, again with the exception of core PS1772-8 (Table 4).

The ^{10}Be rain rates show a positive correlation with the biogenic opal rain rates and, to a lesser extent, with the Ba_{bio} rain rates only in cores PS1754-1 and PS2082-2 north of the present position of the APF. In contrast, insignificant or even negative correlations of ^{10}Be rain rates with rain rates of Ba_{bio} and biogenic

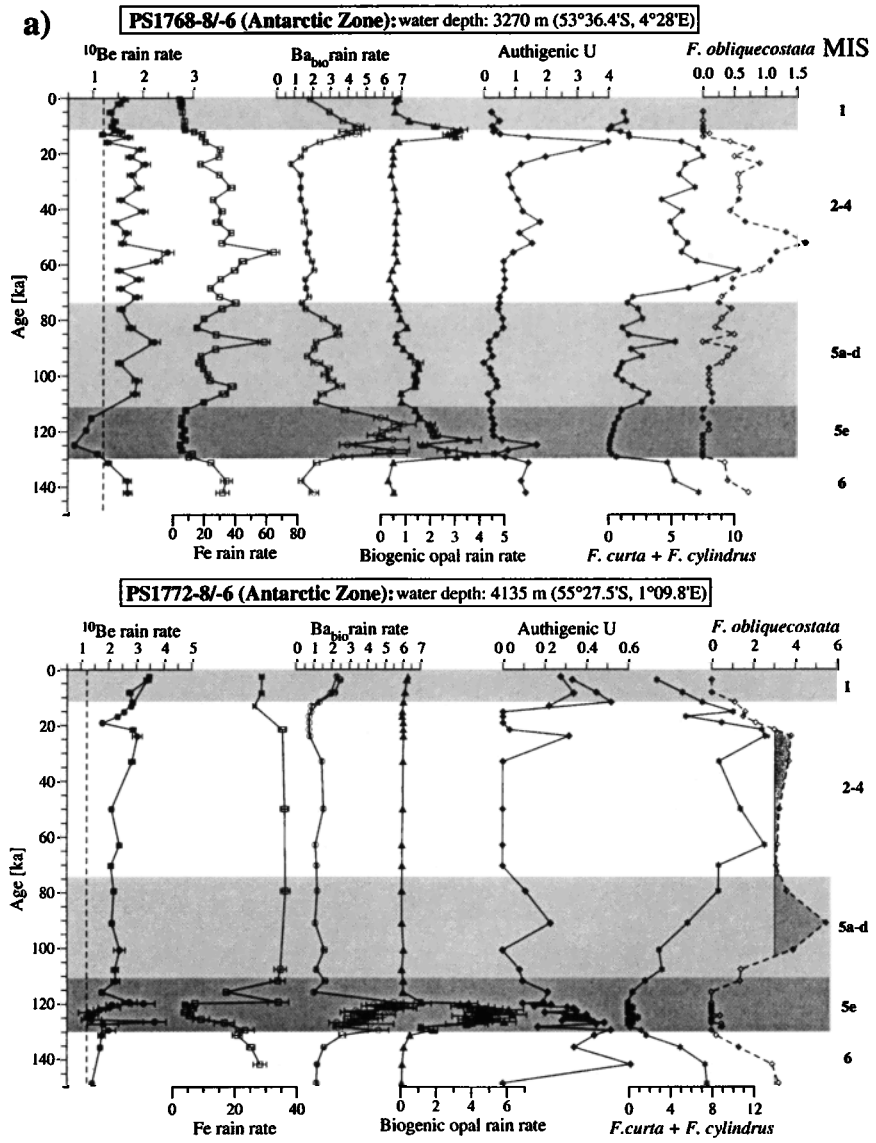

Figure 2. Rain rates ($^{230}Th_{ex}$-normalized accumulation rates) of initial (decay-corrected) ^{10}Be (solid circles), total (detrital) Fe (open squares), preservation-corrected Ba_{bio} (open circles), and biogenic opal (triangles) against age (ka). The rain rates of ^{10}Be are given in 10^9 atoms per square centimeter and thousand years (10^9 at cm^{-2} kyr^{-1}), Fe and Ba_{bio} are given in mg cm^{-2} kyr^{-1} and biogenic opal is given in g cm^{-2} kyr^{-1}. Authigenic U concentrations are given in ppm (diamonds), and the relative abundances of the sea ice indicating diatom species *F. curta* and *F. cylindrus* (stars) and *F. obliquecostata* (open diamonds and dashed curve) are given in percent. Note the different scales. The shaded area on the plot of core PS1772-8 marks the period of year-round sea ice cover. The dashed vertical lines mark the present day global average ^{10}Be production rate of 1.21 x 10^9 at cm^{-2} kyr^{-1} [*Monaghan et al.*, 1985/86]. The light gray shaded areas mark MIS 1 and 5a-d, and the dark gray shading marks the last interglacial climate optimum MIS 5e. Ages were assigned to the isotope stage boundaries following *Martinson et al.* [1987].

opal are observed in the two cores located south of the present-day APF, where the opal belt is presently located (Table 4). In these two cores the highest rain rates of biogenic opal and Ba_{bio} of 6 g cm^{-2} kyr^{-1} and 7 mg cm^{-2} kyr^{-1}, respectively, occur in the sediment intervals representing MIS 1 and 5e. North of the present APF, maxima in biogenic opal rain rates occurred during MIS 2-4 in accordance with a glacial northward shift of the opal belt by 5° that can be deduced from multiple sedimentary parameters [*Charles et al.*, 1991; *Mortlock et al.*, 1991; *Kumar et al.*, 1995; *Yu et al.*, 1996; *Francois et al.*, 1997; *Asmus et al.*, 1999]. An overall drop of the opal rain rates by a factor of 5 is observed in the two northernmost cores, whereas the overall Ba_{bio} rain rate shows a less pronounced drop by a factor of 2-3 only in core PS2082-1 (43°S). This difference might at least partly be ascribed to a low opal preservation efficiency in core PS1754-1, which shows low bulk rain rates and even winnowing during MIS 3-5. In this same core a maximum Ba_{bio} rain rate of 9.5 mg cm^{-2} kyr^{-1} is observed for the MIS 3 section, which is higher than any other values in the cores of this study. This value, however, has to be considered with some caution owing to its proximity to water depths which are saturated for barite [*Monnin et al.*, 1999] and because MIS 3 in this core is also the section showing the

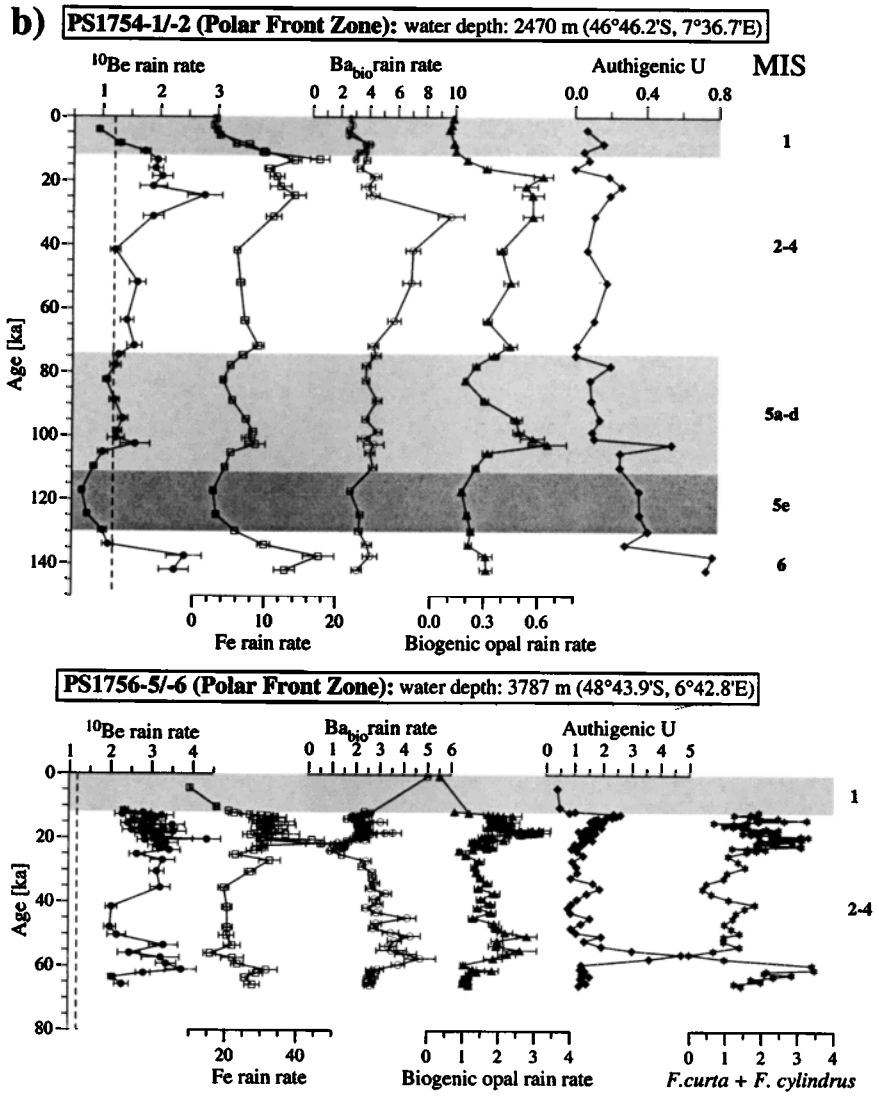

Figure 2. (continued)

strongest winnowing effects and it may be argued that the rain rates in this section are too high due to an overcorrection for sediment redistribution caused by a preferential removal of the fine-grained ($^{230}Th_{ex}$-enriched) fraction [*Frank et al.*, 1996].

Pronounced maxima of authigenic U concentration of up to 5 ppm are observed during glacial MIS 2-4 and 6 in cores PS1768-8, PS1756-5, and PS2082-1. In the core sections corresponding to interglacial MIS 1 and 5, authigenic U concentrations are generally between 0 and 0.5 ppm. In cores PS1754-1 and PS1772-8, only negligible amounts of authigenic U (< 0.5 ppm) are observed. In core PS1756-5 the Ba_{bio} rain rate in the last glacial does not reproduce the maxima in other proxies such as ^{10}Be and biogenic opal rain rates and authigenic U concentration but rather shows a minimum which is apparently due to remobilization of Ba.

In core PS2082-1, rain rates of Ba_{bio} and biogenic opal are overall much lower than farther south, but nevertheless, biogenic opal shows coherent maxima with ^{10}Be rain rates and authigenic U during MIS 2-4 and 6. The Ba_{bio} rain rate does not clearly follow this pattern as evidenced by the reflection of highest maxima of biogenic opal rain rate and authigenic U concentration by sharp minima in Ba_{bio} rain rates at the end of MIS 2 and 6. This confirms the value of authigenic U for indicating Ba remobilization.

In view of the importance of sea ice occurrence for the spatial and temporal pattern of export productivity we compare our particle flux proxies with estimations of past variations of sea ice distribution (Figure 2). Relative abundances of > 3% of the sea ice indicator taxa combined with collapsed sedimentations rates (mainly caused by inhibition of biogenic particle flux) indicate year-round presence of sea ice during MIS 2-4, the upper portion of MIS 5 and MIS 6 at the most southerly located site (core PS1772-8). The occurrence of *F. curta* and *F. cylindrus* in abundances above 3% in core PS1768-8 reflects winter sea ice occurrence in the presently year-round sea ice-free northern Antarctic Zone (AZ) during MIS 2-4 and 6. The low abundance or absence of the diatom sea ice indicators during the MIS 5e in PS1772-8 and during most of MIS 5 in PS1768-8 is interpreted

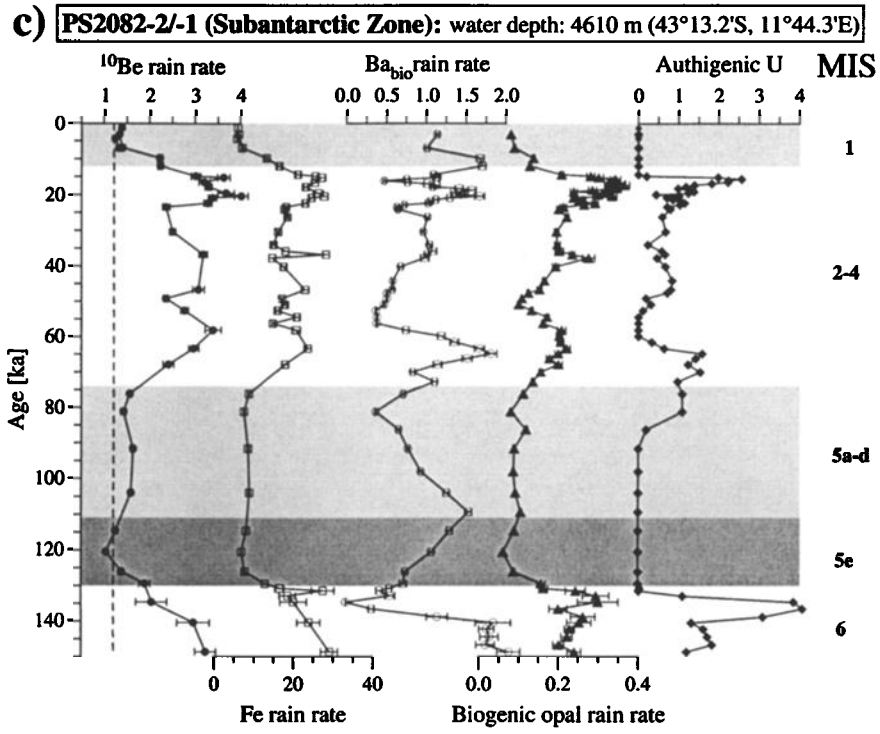

Figure 2. (continued)

to reflect year-round sea ice-free conditions and thus a distinct reduction of the sea ice distribution compared to the present day. During MIS 5e, average summer surface water temperatures in the northern AZ have been estimated to be ~2.5°C higher than present [*Zielinski et al.*, 1998]. In core PS1756-5 farther north the relative abundances of the sea ice diatoms are generally lower (maxima of 4%), but there is, nevertheless, evidence for the presence of winter sea ice during MIS 2 and 4 at this location. The two cores, PS1754-1 and PS2082-1, farther north do not contain significant amounts of the diatom sea ice proxies, which indicates that the sea ice did not reach this zone of the ACC during the recorded time interval.

5. Discussion

In sediment cores from the present PFZ, which represents the approximate position of the opal belt during the Last Glacial Maximum, ^{10}Be and Fe rain rates correlate well with other proxies, such as $^{231}Pa_{ex}/^{230}Th_{ex}$, opal rain rate, and authigenic uranium concentration (Table 4), which all show pronounced maxima during glacial periods [*Kumar*, 1994; *Kumar et al.*, 1995; *Asmus et al.*, 1999]. This has been interpreted as a consequence of increased export productivity linked to fertilization of the nutrient-enriched surface waters by dissolved Fe originating from increased glacial dust fluxes [*Kumar et al.*, 1995]. Time series of Fe rain rates obtained from cores located south of the present APF, where the opal belt has been located during MIS 1 (probably back to ~14.5 ka) and MIS 5e, generally show a similar pattern of glacial maxima and interglacial minima (Figures 2 and 5), indicating enhanced glacial dust fluxes. Time series of ^{10}Be rain rates (cores PS1768-8 in this study, and RC13-259 and RC13-271 of *Kumar* [1994]) and authigenic U concentrations (cores PS1768-8 and RC13-271) south of the APF follow this pattern of the detrital proxy time series. In contrast, the time series of biogenic opal and Ba_{bio} rain rates as well as $^{231}Pa_{ex}/^{230}Th_{ex}$ in the area south of the present APF [*Kumar*, 1994; *Kumar et al.*, 1995; *Francois et al.*, 1997; this study] generally show a different pattern with maximum values during deglacial and interglacial periods. If eolian dust-induced Fe fertilization is the explanation for the good correspondance between all proxies north of the present APF (Table 4), the question arises why this is not the case south of the APF and why ^{10}Be rain rates do not reflect the interglacial maxima in export productivity indicated by the proxies above.

5.1. Export Productivity Information From Rain Rates of Biogenic Opal and Ba_{bio} and $^{231}Pa_{ex}/^{230}Th_{ex}$

There is a possibility that the biogenic opal and Ba_{bio} rain rates and $^{231}Pa_{ex}/^{230}Th_{ex}$ do not give a correct reconstruction of opal-based export paleoproductivity south of the APF but might be biased. Ba_{bio} and biogenic opal rain rates are influenced by effects of preservation and diagenesis after their deposition with, however, one fundamental difference. High bulk accumulation rates (and thus also sediment focusing) are generally believed to promote biogenic opal and Ba_{bio} preservation in sediments owing to shorter periods of contact with undersaturated bottom waters. Those conditions of high sedimentation rates lead to a high preservation efficiency of biogenic opal but at the same time to the devolopment of reducing or suboxic conditions in the subsurface sediment which cause Ba remobilization, a process traced by the simultaneous deposition of authigenic U.

The $^{231}Pa_{ex}/^{230}Th_{ex}$ signal may represent the position of the opal belt rather than increased interglacial opaline particle fluxes due to the relationship of this ratio to opal content and its reduced

Table 4. Correlation Coefficients Between the Proxy Time Series[a]

	Biogenic Opal	Authigenic U	^{10}Be	Ba_{bio}	Fe	Al_2O_3
			PS1772-8/-6			
Biogenic Opal	1					
Authigenic U	0.43[b]	1				
^{10}Be	-0.27	-0.04	1			
Ba_{bio}	0.80[b]	0.36	-0.11	1		
Fe	-0.87[b]	-0.30	0.34	-0.60[b]	1	
Al_2O_3	-0.78[b]	-0.47[b]	0.18	-0.71[b]	0.83[b]	1
			PS1768-8/-1			
Biogenic Opal	1					
Authigenic U	-0.27	1				
^{10}Be	-0.47[b]	-0.01	1			
Ba_{bio}	0.81[b]	-0.31	-0.66[b]	1		
Fe	-0.56[b]	0.16	0.74[b]	-0.64[b]	1	
Al_2O_3	-0.60[b]	0.15	0.76[b]	-0.71[b]	0.91[b]	1
			PS1756-5/-6			
Biogenic Opal	1					
Authigenic U	0.30[b]	1				
^{10}Be	0.06	-0.02	1			
Ba_{bio}	0.10	0.34[b]	-0.18	1		
Fe	0.26	-0.03	0.58[b]	-0.52[b]	1	
Al_2O_3	0.28	-0.33	0.37	-0.66[b]	0.86[b]	1
			PS1754-1/-2			
Biogenic Opal	1					
Authigenic U	0.08	1				
^{10}Be	0.44	0.22	1			
Ba_{bio}	0.50[b]	-0.11	0.17	1		
Fe	0.46[b]	0.27	0.91[b]	0.14	1	
Al_2O_3	0.60[b]	0.18	0.88[b]	0.17	0.88[b]	1
			PS2082-1/-3			
Biogenic Opal	1					
Authigenic U	0.54[b]	1				
^{10}Be	0.85[b]	0.42	1			
Ba_{bio}	0.17	-0.03	0.29	1		
Fe	0.82[b]	0.46[b]	0.95[b]	0.22	1	
Al_2O_3	0.83[b]	0.52[b]	0.93[b]	0.32	0.88[b]	1

[a]Correlation coefficients (r) between the time series of the rain rate proxies and the authigenic U concentrations.
[b]Correlations which are significant at the 99 % level.

sensitivity to mass flux in the presence of opal in the Atlantic sector of the Southern Ocean [*Walter et al.*, 1997]. This results in high sedimentary $^{231}Pa_{ex}/^{230}Th_{ex}$ ratios in areas such as the Weddell Sea, although particle fluxes are overall very low [*Walter et al.*, 1997, 1999]. Conversely, however, if sedimentary $^{231}Pa_{ex}/^{230}Th_{ex}$ ratios are found to be low, this implies that particle flux was low as well as that biogenic opal cannot have been a major component. Thus support for the validity of the interpretation of the observed pattern of opal rain rates south of the APF in terms of export productivity variations comes from a comparison of the $^{231}Pa_{ex}/^{230}Th_{ex}$ ratios and the opal rain rates [*Kumar*, 1994; *Kumar et al.*, 1995]. Coinciding low opal rain rates and $^{231}Pa_{ex}/^{230}Th_{ex}$ ratios are observed for the glacial sediment sections south of the APF, for the interglacial sections north of the APF, and throughout the cores north of the Subantarctic Front (SAF) (RC15-94 and V22-108) [*Kumar*, 1994; *Kumar et al.*, 1995], demonstrating that those periods of low opal rain rates are not a consequence of low preservation efficiency but reflect low opal productivity. Thus, following further the rationale that coherent results derived from Ba_{bio} and biogenic opal rain rates provide a reliable estimate of export paleoproductivity in the absence of authigenic U [*Francois et al.*, 1997; *McManus et al.*, 1998], the results and the interpretation of a higher interglacial than glacial productivity south of the APF presented here and in other studies [*Kumar*, 1994; *Kumar et al.*, 1995; *Francois et al.*, 1997; *Anderson et al.*, 1998] are considered reliable. In addition, the evidence from $^{231}Pa_{ex}/^{230}Th_{ex}$ and opal rain rates [*Kumar et al.*, 1995] suggests that the opal belt did not extend north of the present SAF (~45°S) during MIS 2 and 6.

5.2. The ^{10}Be Rain Rates: Proxy for Export Productivity?

To explain the apparent discrepancy between ^{10}Be rain rates and the other productivity proxies south of the present location of the APF, we suggest a combination of water column stratification, sea ice cover, and a strong affinity of ^{10}Be to clay minerals with key evidence coming from core PS1768-8. At this location the sampling resolution allows a detailed view at the timing of events between 22 and 5 ka (Figure 3). The detrital Fe

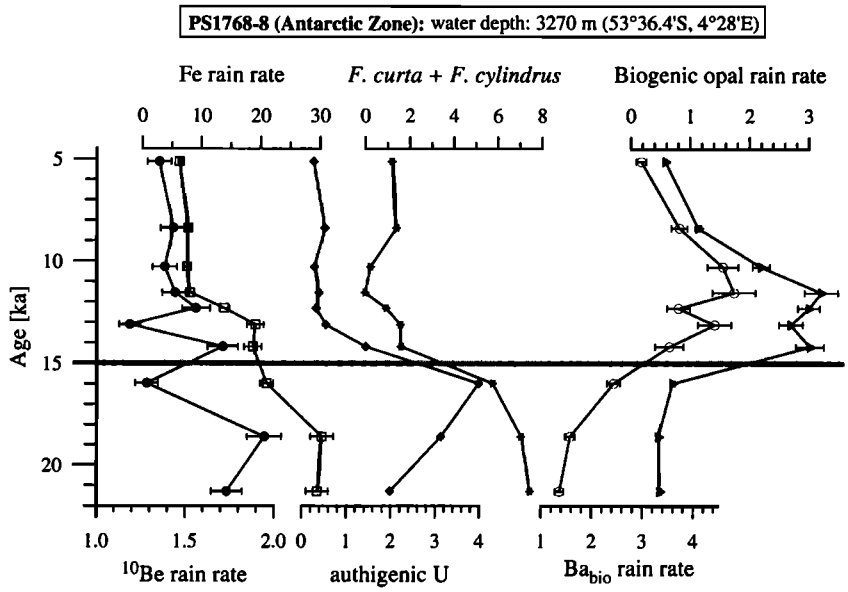

Figure 3. Blowup of all proxies decribed above for the period between 5 and 22 ka in core PS1768-8 from the northern AZ. Symbols and units are the same as in Figure 2. The horizontal line at 15 ka marks the pronounced increase in biogenic opal and Ba_{bio} rain rates linked to a retreat of sea ice as documented by the decrease of the sea ice-indicating diatom abundances and the end of water column stratification as evidenced by the decrease in authigenic U.

supply during the last glacial was a factor of ~4 higher than during interglacials and was not accompanied by increased biogenic opal rain rates. We argue that similar to the Weddell Sea, where organic carbon production and diatom export productivity were shown to be limited in areas with annual and seasonal sea ice cover [*Schlüter*, 1991; *Abelmann and Gersonde*, 1991; *Smetacek et al.*, 1992; *Gersonde and Zielinski*, 2000], the presence of sea ice and an efficient shallow remineralization during MIS 2-4 and 6 at the location of PS1768-8 have contributed to a low export productivity. In addition, there was an increased stratification of the water column south of the present APF (~50°S) which caused a restricted nutrient supply to the surface waters [*Francois et al.*, 1997]. At 15 ka the winter sea ice occurrence rapidly disappeared as documented by the sharp drop in the abundance of the diatom species *F. curta* and *F. cylindrus*. An exactly contemporaneous decrease in authigenic U from 4 to ~0.5 ppm points to an end of the glacial stratification of the water column and a restart of the upwelling and vertical water mass exchange, causing increased O_2 supply to the deep water as suggested by *Francois et al.* [1997] on the basis of nitrogen isotopes. The efficient transfer of nutrients and dissolved silica to the surface waters started again and led to a pronounced increase of opal productivity mirrorred by high rain rates of Ba_{bio}, both starting at ca. 15 ka. In contrast, the rain rates of Fe and ^{10}Be show exactly the opposite trend. They decreased more or less continuously from about ~18 to 12 ka. A similar overall pattern is observed for all proxies at the transition from glacial MIS 6 to interglacial MIS 5e (134-126 ka).

We suggest the following scenario to explain the pattern of the ^{10}Be and Fe rain rates. Seasonal or year-round occurrence of sea ice and water column stratification would restrict neither the availability of ^{10}Be nor the availability of detrital particles of aeolian origin for the sedimentary record on timescales of hundreds to thousands of years. However, owing to greatly reduced production and export of biosiliceous particles, detrital particles became the most abundant type of particle available for ^{10}Be scavenging in the water column south of the APF during glacials, as suggested by the data of core PS1768-8 (Figure 3). This is also supported by the fact that fluctuations in the rain rates of ^{10}Be and Fe in this core match quite well during glacial stages 2-4, for example, in the pronounced maximum at 55 ka, whereas biogenic opal rain rates have remained constantly at low values, consistent with water column stratification, a shallow remineralization and sea ice cover (Figure 2a). In contrast to the situation south of the present APF, the surface waters north of the APF were mostly year-round ice-free during the last glacial, and the water column was not stratified [*Francois et al.*, 1997], giving way to an unrestricted response of export productivity to iron fertilization and hence to a positive correlation of all potential productivity proxies examined [*Kumar*, 1994; *Kumar et al.*, 1995; this study], except for the Ba_{bio}, which is biased in the sections containing authigenic U.

Despite the apparent affinity of ^{10}Be to detrital material, there is also clear evidence for scavenging of ^{10}Be by biogenic opal, as previously found in other studies [*Lao et al.*, 1992b, 1993]. If ^{10}Be rain rates are compared with Fe (detrital) rain rates in the cores south of the APF (including the data presented by *Kumar et al.* [1995]), it is immediately evident that there is no 1:1 relationship as would be expected if detrital particles were exclusively responsible for ^{10}Be scavenging. In particular, the location of the southernmost core PS1772-8 at the present northern winter sea ice edge was year round sea ice-free only during MIS 5e as indicated by the lack of sea ice indicator species and massive contemporaneous peaks of biogenic opal and Ba_{bio} rain rates (Figure 2). The drastic minimum of Fe rain rates in this core during MIS 5e did not coincide with a significant

minimum in ^{10}Be rain rates which we ascribe to enhanced scavenging of ^{10}Be by biogenic opal. A similar pattern is observed at the transition from the last glacial to the Holocene in core RC13-259, also from a location south of the present APF [*Kumar*, 1994]. In this core an interglacial minimum in detrital particle flux coinciding with strong maximum rain rates of biogenic opal, Ba_{bio}, and $^{231}Pa_{ex}$, which started at 15 ka in very good agreement with core PS1768-8, was not accompanied by a minimum in ^{10}Be rain rate but by a small increase after correction for ^{10}Be production rate variations. These observations taken together suggest that the total ^{10}Be rain rate is not a suitable quantitative tracer for biogenic particle flux in the Southern Ocean owing to its sensitivity to both detrital particle flux and biogenic opal flux.

5.3. Authigenic Uranium: Proxy for Export Productivity?

The pattern of glacially increased authigenic U concentrations corresponds well to the patterns of other particle flux proxies ($^{231}Pa_{ex}/^{230}Th_{ex}$, rain rates of ^{10}Be, and biogenic opal) north of the present-day APF. This finding led *Kumar et al.* [1995] to the suggestion that authigenic U deposition in the Atlantic sector of the ACC has mainly been controlled by C_{org} flux and thus export paleoproductivity. A contribution to this authigenic U deposition by decreased glacial O_2 levels of Southern Ocean deep water was dismissed on the basis of a missing glacial authigenic U enrichment in core RC13-259 [*Kumar et al.*, 1995; *Anderson et al.*, 1998]. The concentrations of authigenic U are, however, as mentioned in section 2, a function of three parameters: C_{org} supply, bulk sedimentation rate (and thus also focusing) and deep water oxygen content. All last glacial authigenic U enrichments presented in the study of *Kumar et al.* [1995] and in this study coincide with sediment focusing, which obviously contributed strongly to the U accumulation. The preferential selection of coring locations from sites with high sedimentation rates is the reason why we observe focused sediments in almost all cores [*Frank et al.*, 1996]. In addition, it is important to note that the widespread occurrence of focused MIS 2 sediments in the study area is probably due to a change in bottom water circulation patterns [*Frank et al.*, 1999]. Given that the integrated focusing over an ocean basin has to be 1, the authigenic U from the currently available set of cores cannot be used for any balances of authigenic U deposition and, consequently, biogenic particle flux in the study area during MIS 2. In contrast to these focusing-dominated sediments, *Francois et al.* [1997] showed records of two cores from the Indian sector of the Southern Ocean where glacial authigenic U enrichments are present, although none of the inferred productivity proxies indicated an increased C_{org} flux and although glacial sediment focusing was either negligible or at least lower than during the following interglacial, which is only explainable by lowered O_2 levels of the bottom water.

The data of this study corroborate the complex relationships leading to the precipitation and preservation of authigenic U. Whereas glacial increases in authigenic U are found in most cores at or north of the present-day APF, there is no evidence in core PS1754-1, which is clearly located in the area of the glacial opal belt. The sediments recovered at this site have a relatively high porosity, and sedimentation rates during MIS 2-5 were very low due to winnowing (Table 3) [*Frank et al.*, 1996], which probably prevented authigenic U deposition at this location during MIS 2. Alternatively, some authigenic U may have initially been there

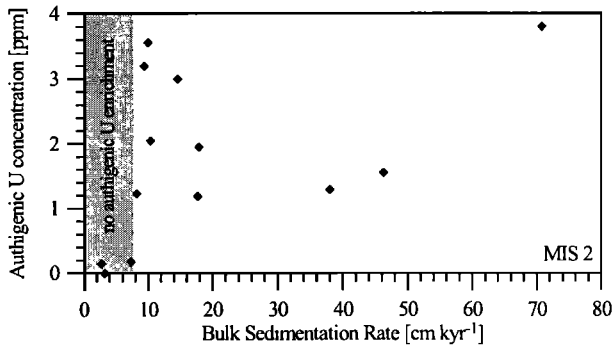

Figure 4. Average authigenic U concentration (ppm) versus sedimentation rate (cm kyr^{-1}) for all MIS 2 sections of the cores of this study and those of *Kumar et al.* [1995] and *Koschmieder* [1996]. The shaded area marks the range of a cutoff sedimentation rate of 8 cm kyr^{-1} below which no deposition of authigenic U occurred.

and been removed by postdepositional remobilization, taking into account the presently high pore water oxygen penetration depths between 30 and > 50 cm in most cores recovered from the eastern Atlantic sector of the ACC [*Rutgers van der Loeff and Berger*, 1991; M. Schlüter, personal communication, 1999].

Low sedimentation rates during the last 100 kyr are also responsible for the lack of glacial authigenic U deposition and preservation in core PS1772-8 in the AZ for which the oxygen penetration depth is presently higher than 50 cm [*Rutgers van der Loeff and Berger*, 1991; M. Schlüter, personal communication, 1999]. The absence of glacial authigenic U enrichment in core RC13-259, with a sedimentation rate of 7.5 cm kyr^{-1} and focusing factor ~1 during MIS 2, implies a low export production at this position. The argument of *Kumar et al.* [1995] mentioned above that the record of this core constitutes a proof against lowered bottom water O_2 levels may have to be reconsidered in the light of the evidence for such reduced bottom water oxygen levels in the glacial Indian Ocean [*Francois et al.*, 1997]. We suggest that the combined effects of sediment accumulation rate and low bottom water O_2 level, on the one hand, were not sufficient to compensate for the very low C_{org} flux, indicated by the very low C_{org}/biogenic opal ratios in this area [*Schlüter et al.*, 1998; M. Schlüter, personal communication, 1999], on the other, and thus not sufficient to cause accumulation of authigenic U in core RC13-259. A comparison of all available MIS 2 sediment sections from the Atlantic sector of the Southern Ocean (Figure 4) shows that RC13-259 is just at the border of a cutoff sedimentation rate of 8 cm kyr^{-1}, below which no deposition of authigenic U occurred. This relationship may hold despite lowered O_2 levels. Above this rate, apparently enough organic carbon was buried to cause the suboxic conditions required for authigenic U accumulation. For the Holocene data such a transition is not visible, and the authigenic U concentrations remained close to the detection limit.

The other two available cores from the AZ (PS1768-8 and RC13-271) show enrichments of authigenic U during glacials, mainly as a consequence of the high focusing intensities, which do not coincide with the peaks of other proxies, such as $^{231}Pa_{ex}/^{230}Th_{ex}$ and rain rates of opal. In the case of these two cores the present oxygen penetration depth is ~30 cm [*Rutgers van der Loeff and Berger*, 1991], but the bulk sedimentation rate

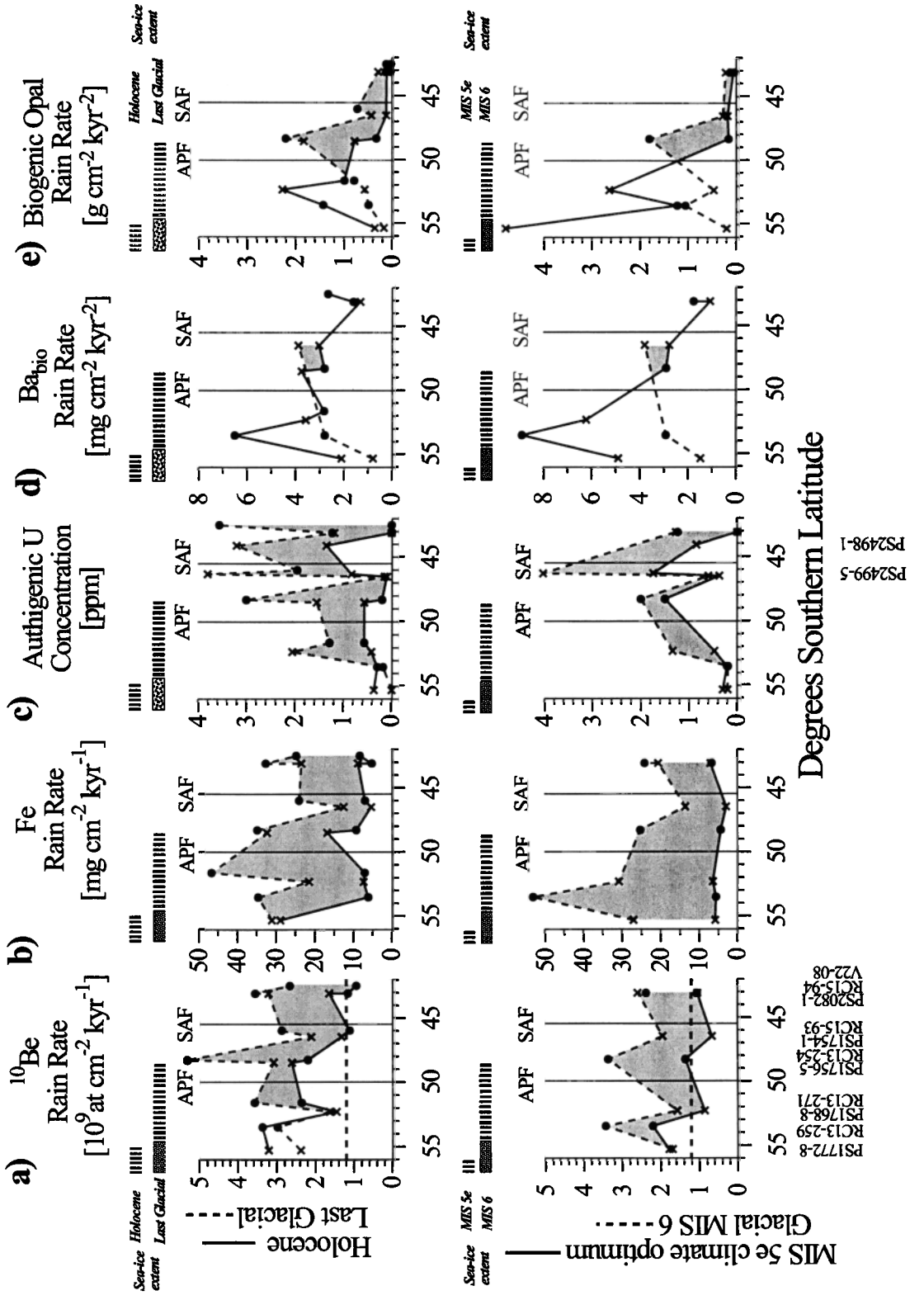
a) ^{10}Be Rain Rate [10^9at cm^{-2} kyr^{-1}]
b) Fe Rain Rate [mg cm^{-2} kyr^{-1}]
c) Authigenic U Concentration [ppm]
d) Ba_{bio} Rain Rate [mg cm^{-2} kyr^{-2}]
e) Biogenic Opal Rain Rate [g cm^{-2} kyr^{-2}]
Sea-ice extent
Holocene
Last Glacial
MIS 5e
MIS 6
APF
SAF
Holocene ——
Last Glacial - - - -
MIS 5e climate optimum ——
Glacial MIS 6 - - - -
PS1772-8
RC13-259
PS1768-8
RC13-271
PS1756-5
RC13-254
PS1754-1
RC15-93
PS2082-1
RC15-94
V22-08
PS2499-5
PS2498-1
Degrees Southern Latitude

Figure 5.

in both cores has been high enough to allow for the deposition of authigenic U and prevent it from postdepositional removal. Similarly, cores containing glacial authigenic U enrichments without significant enrichment of other biogenic particle flux proxies ($^{231}Pa_{ex}/^{230}Th_{ex}$ and rain rates of opal) are found north of the SAF (RC15-94 and V22-108), which is attributed to intense sediment focusing.

We conclude that despite the fact that C_{org} flux has been an important factor for the enrichment of authigenic U in Southern Ocean sediments, particularly during glacials in the present PFZ, the apparent sensitivity of authigenic U accumulation to bulk sedimentation rate and sediment focusing, on the one hand, and lowered bottom water oxygenation, on the other, suggests that authigenic U is not a suitable proxy for export paleoproductivity in the eastern Atlantic sector of the Southern Ocean.

5.4 Reconstruction of Export Productivity

We combined the average glacial and interglacial rain rates of all parameters of this study with the results obtained by *Kumar* [1994] and *Kumar et al.* [1995] which show a very good internal consistency in all parameters (Figure 5). In view of the shortcomings of each proxy discussed before, the rationale of this reconstruction cannot be to come up with unambiguous quantitative estimates of export paleoproductivity. Rather the estimates for the main interglacial export areas south of the present APF are compared with those for the main glacial export areas, which were shifted north of the present APF. In doing so, we expect that the systematic underestimation of the ^{230}Th-normalized rain rates, which is caused by an additional import of ^{230}Th from the Weddell Sea into this area [*Rutgers van der Loeff and Berger*, 1993; *Walter et al.*, 2000], mostly cancels out. We also assume that opal dissolution and C_{org}/biogenic opal ratios have remained constant within the moving opal belt on glacial-interglacial timescales. For opal dissolution this assumption has recently been strengthened by the finding that dissolution may modulate opal rain rates in the Southern Ocean but not as a primary factor [*Pondaven et al.*, 2000]. The approach of this study will thus provide the possibility to assess whether overall glacial export productivity in the eastern Atlantic sector of the Southern Ocean was higher than during interglacials or not. Such a productivity comparison has crucial implications for the question whether the glacial Southern Ocean was a potential sink of atmospheric CO_2 or not. As discussed before, we do not consider ^{10}Be rain rates and authigenic U reliable proxies for biogenic particle flux and will therefore base our synthesis on the rain rates of biogenic opal and Ba_{bio} (in those sections without authigenic U) complemented by other available paleo-environmental parameters (sea ice extent, water column stratification, and Fe fertilization).

Higher interglacial than glacial values of the rain rates of Ba_{bio} and biogenic opal are observed for most of the cores from the AZ whereas in the PFZ north of the present-day position of the APF the opposite is observed (Figures 5d and 5e). The overall comparison of the interglacial maxima of biogenic opal rain rates south of the present APF with the glacial maxima north of the APF shows either similar or even somewhat higher interglacial than glacial values, in particular when comparing MIS 6 and 5e. In the case of the only three valid glacial Ba_{bio} rain rates (cores PS1772-8, RC13-259, and PS1754-1) it has to be assumed that the absence of authigenic U in these core sections is a primary feature and has not been caused by postdepositional burn-down. We therefore suggest that even these data have to be considered with some caution. Biogenic opal rain rates appear to be the most reliable proxy in view of the rationale of comparing proxy data from the interglacial position of the opal belt south of the APF with those from the glacial position north of the APF and display very systematic changes and a nearly perfect mirror image of each other for MIS 1 and 2 (Figure 5e). Translating this pattern into a correct quantitative comparison of the overall amount of Southern Ocean glacial/interglacial opal rain rates would require a precise knowledge of the exact spacial extent of the glacial and interglacial opal belt which is, unfortunately, not yet available.

From these results we, nevertheless, can infer that the increased input of aeolian dust and a potentially linked fertilization of the surface waters during the last glacial [*Martin*, 1990; *Kumar et al.*, 1995] may only have resulted in increased export paleoproductivity north of the present-day position of the APF. For the area south of the APF we suggest that a seasonal or, in the case of PS1772-8, even year-round sea ice cover during the last glacial together with a shallow remineralization [*Usbeck and Schlitzer*, 1999; *Rutgers van der Loeff and Hoppema*, 1999] and an increased stratification of the water column [*Francois et al.*, 1997] prevented a positive response of opal-dominated export fluxes to such fertilization. The possible Fe fertilization north of the APF did, however, apparently not result in a significantly

Fig. 5: Comparison of the average rain rates for the last glacial and present interglacial as well as the penultimate glacial and interglacial MIS 5e as a function of latitude in the eastern Atlantic sector of the Southern Ocean (the results of this study (crosses) are shown together with the data from *Kumar* [1994] and *Kumar et al.* [1995] (solid circles): (a) ^{10}Be; (b) total (detrital) Fe; (c) concentrations of authigenic U; (d) preservation-corrected Ba_{bio} only for those sections where authigenic U concentrations are below 0.5 ppm, which is considered to be the uncertainty of the calculation of authigenic U from the mean crustal U/Th ratio; and (e) biogenic opal. The solid lines mark the average values for the present MIS 1 (Holocene) (except for PS1768-8, where it reflects the average value for the last 14.5 kyr) and the MIS 5e climate optimum (120-125 ka), and the dashed lines mark the average last glacial MIS 2 and MIS 6 values. The vertical lines at 50° and 45.5°S represent the average present-day positions of the APF and SAF, respectively. The dashed horizontal line in Figure 5a is the present-day global average ^{10}Be production rate [*Monaghan et al.*, 19985/86]. The shaded areas mark periods where glacial values are higher than the corresponding interglacial values. A spike calibration problem at the Lamont group rendered their ^{10}Be results by *Kumar* [1994] and *Kumar et al.* [1995] 40% too high (*R.F. Anderson*, personal communication, 1999). The data taken from these sources were adjusted to this offset and were additionally corrected for cosmogenic production rate variations caused by variations of the geomagnetic field intensity [*Guyodo and Valet*, 1996; *Frank et al.*, 1997] to allow a direct comparison. In Figure 5c authigenic U concentrations of two more cores (PS2499-5, 46°31'S, 15°20'W and PS2498-1, 44°10'S, 14°14'W) from *Koschmieder* [1996] are added. Above the transect the approximate extent of sea ice cover is plotted. The solid bar indicates year-round sea ice cover during the last glacial MIS 2 and MIS 6, whereas the broken bar marks the approximate extent of seasonal (winter) sea ice. Note that the southernmost location of core PS1772-8 was covered by seasonal sea ice during the Holocene, whereas it was year-round ice-free during MIS 5e.

higher glacial productivity than during the interglacials south of the APF.

We applied the algorithm given by *Francois et al.* [1995] to estimate export productivities from Ba_{bio} rain rates, although there are additional uncertainties related to variable Ba_{bio}/C_{org} ratios [*Dymond and Collier*, 1996] and variable preservation efficiencies [*Kumar et al.*, 1996; *McManus et al.*, 1999] derived from sediment trap studies. For MIS 1 we obtain values of 10-20 g C m^{-2} yr^{-1} for the area of the present APF. This is in relatively good agreement with export productivity at 100 m water depth of ~15 g C m^{-2} yr^{-1} determined from sediment traps in the same area [*Wefer and Fischer*, 1991], which were, however, not corrected for collection efficiency. Results based on ^{234}Th from the same area showed values ~26 g C m^{-2} yr^{-1} at 100 m water depth (M.M. Rutgers van der Loeff et al., Steady summer production and a sudden spring bloom make a comparable contribution to carbon and opal export near the Antarctic Polar Front, SE Atlantic, submitted to *Deep Sea Res., Part II*, 2000) Maximum levels of export productivity for the entire transect are calculated from the MIS 3 Ba_{bio} rain rates of core PS1754-1. These are, as discussed before, probably somewhat too high but reach ~50 g C cm^{-2} kyr^{-1}, which is comparable to the highest interglacial maxima south of the APF (~30 C cm^{-2} kyr^{-1} during MIS 5e in cores PS1772-8 and PS1768-8), but, by far, not as high as in coastal upwelling high productivity areas.

In accordance with *Francois et al.* [1997] this implies that an increased export productivity of the glacial Southern Ocean cannot serve as a viable process to lower glacial atmospheric CO_2. Nevertheless, our data, in particular the high glacial authigenic U concentrations in core PS1768-8, support the view that a stratification of the Southern Ocean water column south of the APF during glacials, possibly linked to sea ice cover, diminished the "CO_2 leak" to the atmosphere [*Francois et al.*, 1997]. A similar mechanism, which is also consistent with our U data and the reconstructions of sea ice extent [*Gersonde and Zielinski*, 2000], directly invokes sea ice cover to decrease surface exposure of glacial Southern Ocean deep-water and thus to decrease the CO_2 transfer to the atmosphere [*Stephens and Keeling*, 2000; *Elderfield and Rickaby*, 2000]. Alternatively, a globally increased glacial export productivity linked to a global increase in dust flux and involving the oceanic nitrogen cycle may have played a role [*Broecker and Henderson*, 1998].

There are a lot of questions left. One is, for example, whether the biogenic opal rain rates represent a reliable proxy for export paleoproductivity or whether there was a glacial decoupling of C_{org} and biogenic opal rain rates [*Kumar et al.*, 1995; *Anderson et al.*, 1998]. Evidence for a present decoupling of C_{org} and biogenic opal accumulation within the Southern Ocean has been shown by lower C_{org}/biogenic opal ratios in the eastern Atlantic sector than in the Scotia Sea and Weddell Sea areas [*Schlüter et al.*, 1998; M. Schlüter, personal communication, 1999]. On glacial-interglacial timescales the difference between the moderately increased glacial opal rain rates and the strongly increased glacial ^{10}Be, $^{231}Pa_{ex}/^{230}Th_{ex}$, and authigenic U accumulation rates was initially suggested to provide evidence for such a decoupling [*Kumar et al.*, 1995]. The results of our study on ^{10}Be rain rates and authigenic U and the results of *Walter et al.* [1997, 1999] on $^{231}Pa_{ex}/^{230}Th_{ex}$ apparently do not support the use of those three proxies to reconstruct export paleoproductivity and thus also weaken the argument on decoupling of biogenic opal and C_{org} on glacial-interglacial timescales. A comparison of biogenic opal and C_{org} rain rates themselves [*Anderson et al.*, 1998] also suggests lower biogenic opal to C_{org} ratios during glacials north of the APF than during interglacials south of the APF. In view of the effects deduced for the authigenic U signal in this study, however, it is inferred that C_{org} accumulation and preservation have been similarly influenced by intense focusing and lowered glacial bottom water O_2 and must be considered with great caution.

6. Conclusions

Despite the uncertainties that still exist with all potential proxies for export paleoproductivity of this multiproxy approach, the good correspondance of biogenic opal rain rates and those Ba_{bio} rain rates derived from core sections without authigenic U in comparing the interglacial maxima south of the APF and the glacial maxima north of the APF provides evidence that overall glacial export productivity of the Southern Ocean was similar to its values during interglacials. Whereas Fe fertilization may have contributed to glacial maxima in export productivity north of the present position of the APF as mirrored by maxima in most proxies presented, a response of opal export productivity to increased glacial Fe input south of the APF was apparently grossly restricted by water column stratification, sea ice cover, and a shallow remineralization depth. Despite a possible Fe fertilization the glacial opal productivity north of the APF was apparently not higher than during the interglacials south of the APF. It is also inferred that export productivity in the Atlantic sector of the Southern Ocean has, by far, not reached levels of coastal upwelling areas during the past 150 kyr. As a consequence, we suggest that increased export productivity in the Southern Ocean has not contributed to lowered glacial atmospheric CO_2 levels.

There is more work needed to better constrain and quantify the uncertainties associated with every proxy used in this study, such as oxygen levels of the deep water, spacial differences between the proxies in the eastern and western Atlantic sectors of the Southern Ocean, and variability of the relationships between C_{org} and biogenic opal and Ba_{bio}. Multiproxy approaches certainly provide more reliable reconstructions of export paleoproductivity than using single proxies alone, but even this does not necessarily imply that we are close to a quantitative estimate of export paleoproductivity as long as the uncertainties with each of the proxies are too high.

Acknowledgments. This study was supported by grants Ma821/9-1 to -3 from the German Science Foundation. We want to thank Bob Anderson, Niraj Kumar, Roger Francois, Gideon Henderson, and Gerald Haug for numerous constructive discussions which contributed substantially to this work. Jerry McManus, Danny Sigman, and four anonymous reviewers are thanked for their thorough and constructive reviews. M.F. wants to thank in particular R. K. O'Nions and A. N. Halliday for the possibility to finish the work on this study in Oxford and Zürich, repectively. This is SFB 261 contribution No. 7.

References

Abelmann, A., and R. Gersonde, Biosiliceous particle flux in the Southern Ocean, *Mar. Chem., 35*, 503-536, 1991.

Anderson, R.F., Redox behavior of uranium in an anoxic marine basin, *Uranium, 3*, 145-164, 1987.

Anderson, R.F., Y. Lao, W.S. Broecker, S.E. Trumbore, H.J. Hofmann, and W. Wölfli, Boundary scavenging in the Pacific Ocean: A comparison of ^{10}Be and ^{231}Pa, *Earth Planet. Sci. Lett., 96*, 287-304, 1990.

Anderson, R.F., M.Q. Fleisher, P.E. Biscaye, N. Kumar, B. Dittrich, P.W. Kubik, and M. Suter, Anomalous boundary scavenging in the Middle Atlantic Bight: Evidence from ^{230}Th, ^{231}Pa, ^{10}Be and ^{210}Pb, *Deep Sea Res., Part II, 41*, 537-561, 1994.

Anderson, R.F., N. Kumar, R.A. Mortlock, P.N. Froelich, P.W. Kubik, B. Dittrich-Hannen, and M. Suter, Late-Quaternary changes in productivity of the Southern Ocean, *J. Mar. Syst., 17*, 497-514, 1998.

Asmus, T., M. Frank, C. Koschmieder, N. Frank, R. Gersonde, and A. Mangini, Variations of biogenic particle flux in the southern Atlantic section of the Subantarctic Front during the late Quaternary: Evidence from sedimentary $^{231}Pa_{ex}$ and $^{230}Th_{ex}$, *Mar. Geol., 159*, 63-78, 1999.

Bacon, M.P. Glacial to interglacial changes in carbonate and clay sedimentation in the Atlantic estimated from thorium-230 measurements, *Isot. Geosci., 2*, 97-111, 1984.

Bacon, M.P., and J.N. Rosholt, Accumulation rates of ^{230}Th and ^{231}Pa and some transition metals on the Bermuda Rise, *Geochim. Cosmochim. Acta, 46*, 651-666, 1982.

Bard, E., B. Hamelin, R.G. Fairbanks, and A. Zindler, Calibration of the ^{14}C timescale over the past 30,000 years using mass spectrometric U-Th ages from Barbados corals, *Nature, 345*, 405-410, 1990.

Barnes, C.E., and J.K. Cochran, Uranium removal in oceanic sediments and the oceanic uranium balance, *Earth Planet. Sci. Lett., 97*, 94-104, 1990.

Barnola, J.M., D. Raynaud, Y.S. Korotkevich, and C. Lorius, Vostok ice core provides 160,000 year record of atmospheric CO_2, *Nature, 329*, 408-414, 1987.

Behrenfeld, M.J., A.J. Bale, Z.S. Kolber, J. Aiken, and P.G. Falkowski, Confirmation of iron limitation of phytoplankton photosynthsis in the equatorial Pacific Ocean, *Nature, 383*, 508-511, 1996.

Bishop, J.K.B., The barite-opal-organic carbon association in oceanic particulate matter, *Nature, 332*, 341-343, 1988.

Bourlès, D.L., G.M. Raisbeck, and F. Yiou, ^{10}Be and ^{9}Be in marine sediments and their potential for dating, *Geochim. Cosmochim. Acta, 53*, 443-452, 1989a.

Bourlès, D.L., G. Klinkhammer, A.C. Campbell, C.I. Measures, E.T. Brown, and J.M. Edmond, Beryllium in marine pore waters: Geochemical and geochronological implications, *Nature, 341*, 731-733, 1989b.

Broecker, W.S., and G.M. Henderson, The sequence of events surrounding Termination II and their implications for the cause of glacial-interglacial CO_2 changes, *Paleoceanography, 13*, 352-364, 1998.

Broecker, W.S, and T.H. Peng, *Tracers in the Sea*, 690 pp., Lamont Doherty Geological Observatory, Palisades, N. Y., 1982.

Charles, C.D., and R.G. Fairbanks, Glacial to interglacial changes in the isotopic gradients of Southern Ocean surface water, in *The Geological History of the Polar Oceans: Arctic vs. Antarctic*, edited by U. Bleil and J. Thiede, pp. 519-538, Kluwer Acad., Norwell, Mass., 1990.

Charles, C.D., P.N. Froelich, A. Zibello, R.A. Mortlock, and J.J. Morley, Biogenic opal in Southern Ocean sediments over the last 450,000 years: Implications for surface water chemistry and circulation, *Paleoceanography, 6*, 697-728, 1991.

Coale, K.H., et al., A massive phytoplankton bloom induced by an ecosystem-scale iron fertilization experiment in the equatorial Pacific Ocean, *Nature, 383*, 495-501, 1996.

Cochran, J.K., and S. Krishnaswami, Radium, thorium, uranium and Pb-210 in deep-sea sediments and sediment pore waters from the North Equatorial Pacific, *Am. J. Sci., 280*, 849-889, 1980.

Crosta, X., J.-J. Pichon, and L.H. Burckle, Application of the modern analog technique to marine Antarctic diatoms: Reconstruction of maximum sea ice extent at the Last Glacial Maximum, *Paleoceanography, 13*, 284-297, 1998a.

Crosta, X., J.-J. Pichon, and L.H. Burckle, Reappraisal of Antarctic seasonal sea ice at the Last Glacial Maximum, *Geophys. Res. Lett., 25*, 2703-2706, 1998b.

De Angelis, M., N.I. Barkov, V.N. Petrov, Aerosol concentrations over the last climatic cycle (160 kyr) from an Antarctic ice core, *Nature, 325*, 318-321, 1987.

de Baar, H.J.W., J.T.M. de Jong, D.C.E. Bakker, B.M. Löscher, C. Veth, U. Bathmann, and V. Smetacek, Importance of iron for plankton blooms and carbon dioxide drawdown in the Southern Ocean, *Nature, 373*, 412-415, 1995.

Dehairs, F., R. Chesselet, and J. Jedwab, Discrete suspended particles of barite and the barium cycle in the open ocean, *Earth Planet. Sci. Lett. 49*, 528-550, 1980.

Dehairs, F., N. Fagel, A.N. Antia, R. Peinert, M. Elskens, and L. Goeyens, Export production in the Bay of Biscay as estimated from barium – barite in settling material: A comparison with new production, *Deep Sea Res., Part I, 47*, 583-601, 2000.

Diekmann, B., G. Kuhn, A. Mackensen, R. Petschick, D.K. Fütterer, R. Gersonde, C. Rühlemann, and H.-S. Niebler, Kaolinite and Chlorite as tracers of modern and Late Quaternary deep water circulation in the south Atlantic and the adjoining Southern Ocean, in *Use of Proxies in Paleoceanography: Examples from the South Atlantic*, edited by G. Fischer and G. Wefer, pp. 285-313, Springer-Verlag, New York, 1999.

Dymond, J., and R. Collier, Particulate barium fluxes and their relationships to biological productivity, *Deep Sea Res., Part II, 43*, 1283-1308, 1996.

Dymond, J., E. Suess, and M. Lyle, Barium in deep-sea sediment: A geochemical indicator of paleoproductivity, *Paleoceanography, 7*, 163-181, 1992.

Eisma, D., and S.J. van der Gaast, Determination of opal in marine sediments by X-ray diffraction, *Neth. J. Sea Res., 5*, 382-389, 1971.

Elderfield, H., and R.E.M. Rickaby, Oceanic Cd/P ratio and nutrient utilization in the glacial Southern Ocean, *Nature, 405*, 305-310, 2000.

Fischer, G., D. Fütterer, R. Gersonde, S. Honjo, D. Ostermann, and G. Wefer, Seasonal variability of particle flux in the Weddell Sea and its relation to ice cover, *Nature, 335*, 426-428, 1988.

Fleet Numerical Meteorology and Oceanography Detachment, Sea Ice Climatic Atlas, vol. 1, *Antarctic*, 131 pp., Naval Oceanography Command Detachment, Ashville, N. C., 1985.

Francois, R., M.P. Bacon, and D. Suman, Thorium 230 profiling in deep-sea sediments: High-resolution records of flux and dissolution of carbonate in the equatorial Atlantic during the last 24,000 years, *Paleoceanography, 5*, 761-787, 1990.

Francois, R., M.P. Bacon, M.A. Altabet, and L.D. Labeyrie, Glacial/interglacial changes in sediment rain rate in the SW Indian sector of Subantarctic waters as recorded by ^{230}Th, ^{231}Pa, U, and δ^{15}N, *Paleoceanography, 8*, 611-629, 1993.

Francois, R., S. Honjo, S.J. Manganini, and G.E. Ravizza, Biogenic barium fluxes to the deep sea: Implications for paleoproductivity reconstruction, *Global Biogeochem. Cycles, 9*, 289-303, 1995.

Francois, R., M.A. Altabet, E.-F. Yu, D. Sigman, M.P. Bacon, M. Frank, G. Bohrmann, G. Bareille, and L. Labeyrie, Contribution of Southern Ocean surface-water stratification to low atmospheric CO_2 concentrations during the last glacial period, *Nature, 389*, 929-935, 1997.

Frank, M., J.-D. Eckhardt, A. Eisenhauer, P.W. Kubik, B. Dittrich-Hannen, and A. Mangini, Beryllium 10, thorium 230 and protactinium 231 in Galapagos Microplate sediments: Implications for hydrothermal activity and paleoproductivity changes during the last 100,000 years, *Paleoceanography, 9*, 559-578, 1994.

Frank, M., A. Eisenhauer, W.J. Bonn, P. Walter, H. Grobe, P.W. Kubik, B. Dittrich-Hannen, and A. Mangini, Sediment redistribution versus paleoproductivity change: Weddell Sea margin sediment stratigraphy for the last 250,000 years deduced from $^{230}Th_{ex}$, ^{10}Be and biogenic barium profiles, *Earth Planet. Sci. Lett. 136*, 559-573, 1995.

Frank, M., R. Gersonde, M. Rutgers van der Loeff, G. Kuhn, and A. Mangini, Late Quaternary sediment dating and quantification of lateral sediment redistribution applying $^{230}Th_{ex}$: A study from the eastern Atlantic sector of the Southern Ocean, *Geol. Rundsch., 85*, 554-566, 1996.

Frank, M., B. Schwarz, S. Baumann, P.W. Kubik, M. Suter, and A. Mangini, A 200 kyr record of cosmogenic radionuclide production rate and geomagnetic field intensity from ^{10}Be in globally stacked deep-sea sediments, *Earth Planet. Sci. Lett., 149*, 121-129, 1997.

Frank, M., R. Gersonde, and A. Mangini, Sediment redistribution, $^{230}Th_{ex}$-normalization and implications for the reconstruction of particle flux and export paleoproductivity, in *Use of Proxies in Paleoceanography: Examples from the South Atlantic*, edited by G. Fischer and G. Wefer, pp. 409-426, Springer-Verlag, New York, 1999.

Gersonde, R., and U. Zielinski, The reconstruction of late Quaternary Antarctic sea ice distribution: The use of diatoms as a proxy for sea ice, *Palaeogeogr. Palaeoclimatol. Palaeoecol.*, in press, 2000.

Grousset, F.E., P.E. Biscaye, M. Revel, J.-R. Petit, K. Pye, S. Joussaume, and J. Jouzel, Antarctic (Dome C) ice-core dust at 18 k.y. B.P.: Isotopic constraints on origins, *Earth Planet. Sci. Lett., 111*, 175-182, 1992.

Guyodo, Y., and J.-P. Valet, Relative variations in geomagnetic intensity from sedimentary records: The past 200 thousand years, *Earth Planet. Sci. Lett., 143*, 23-36, 1996.

Haug, G., D.M. Sigman, R. Tiedemann, T.F. Pedersen, and M. Sarnthein, Onset of permanent stratification in the subarctic Pacific Ocean, *Nature, 401*, 779-782, 1999.

Hempel, P., and G. Bohrmann, Analyses of

carbonate-free sediment composition and aspects of silica diagenesis in sediments drilled during ODP Leg 115 in the western Indian Ocean (Sites 707, 709 and 711), *Proc. Ocean Drill. Program Sci. Results, 115*, 677-689, 1990.

Henderson, G.M., C. Heinze, R.F. Anderson, and A.M.E. Winguth, Global distribution of the ^{230}Th flux to ocean sediments constrained by GCM modeling, *Deep Sea Res., Part I, 46*, 1861-1893, 1999.

Henken-Mellies, W.U., J. Beer, F. Heller, K.J. Hsü, C. Shen, G. Bonani, H.J. Hofmann, M. Suter, and W. Wölfli, ^{10}Be and ^{9}Be in South Atlantic DSDP site 519: Relation to geomagnetic reversals and to sediment composition, *Earth Planet. Sci. Lett., 98*, 267-276, 1990.

Hofmann, H.J., J. Beer, G. Bonani, H.R. von Gunten, S. Raman, M. Suter, R.L. Walker, W. Wölfli, and D. Zimmermann, ^{10}Be: Half-life and AMS standards, *Nucl. Instrum. Methods Phys. Res.*, Sect. *B, 29*, 32-36, 1987.

Ikehara, M., K. Kawamura, N. Ohkouchi, M. Murayama, T. Nakamura, and A. Taira, Variations of terrestrial input and marine productivity in the Southern Ocean (48°S) during the last two deglaciations, *Paleoceanography, 15*, 170-180, 2000.

Jeandel, C., K. Tachikawa, A. Bory, and F. Dehairs, Biogenic barium in suspended and trapped material as a tracer of export production in the tropical NE Atlantic (EUMELI sites), *Mar. Chem., 71*, 125-142, 2000.

Jung, M., J. Ilmberger, A. Mangini, and K.-C. Emeis, Why some Mediterranean sapropels survived burn-down (and others did not), *Mar. Geol., 141*, 51-60, 1997.

Klinkhammer, G., and M.R. Palmer, Uranium in the oceans, where it goes and why, *Geochim. Cosmochim. Acta, 55*, 1799-1806, 1991.

Knox, F., and M.B. McElroy, Changes in atmospheric CO_2: Influence of marine biota at high latitudes, *J. Geophys. Res., 89*, 4629-4637, 1984.

Koschmieder, C., Zeitlich hochauflösende Rekonstruktion von spätquartären Sedimentationsbedingungen im Südatlantik mit Hilfe von ^{230}Th, M.Sc. thesis, 58 pp., Univ. Heidelberg, Heidelberg, Germany, 1996.

Kumar, N., Trace metals and natural radionuclides as tracers of ocean productivity, Ph.D. thesis, 317 pp., Columbia Univ., New York, 1994.

Kumar, N., R. Gwiazda, R.F., Anderson, and P.N. Froelich, ^{231}Pa/^{230}Th ratios in sediments as a proxy for past changes in Southern Ocean productivity, *Nature, 362*, 45-48, 1993.

Kumar, N., R.F. Anderson, R.A. Mortlock, P.N. Froelich, P.W. Kubik, B. Dittrich-Hannen, and M. Suter, Increased biological productivity and export production in the glacial Southern Ocean, *Nature, 378*, 675-680, 1995.

Kumar, N., R.F. Anderson, and P.E. Biscaye, Remineralization of particulate authigenic trace metals in the Middle Atlantic Bight: Implications for proxies of export production, *Geochim. Cosmochim. Acta, 60*, 3383-3397, 1996.

Labeyrie, L., and J.-C. Duplessy, Change in oceanic ^{13}C/^{12}C ratio during the last 140000 years: High latitude surface water records, *Palaeogeogr. Palaeoclimatol. Palaeoecol., 50*, 217-240, 1985.

Lao, Y., R.F. Anderson, W.S. Broecker, S.E. Trumbore, H.J. Hofmann, and W. Wölfli, Increased production of cosmogenic ^{10}Be during the Last Glacial Maximum, *Nature, 357*, 576-578, 1992a.

Lao, Y., R.F. Anderson, W.S. Broecker, S.E. Trumbore, H.J. Hofmann, and W. Wölfli, Transport and burial rates of ^{10}Be and ^{231}Pa in the Pacific Ocean during the Holocene period, *Earth Planet. Sci. Lett. 113*, 173-189, 1992b.

Lao, Y., R.F. Anderson, W.S. Broecker, H.J. Hofmann, and W. Wölfli, Particulate fluxes of ^{230}Th, ^{231}Pa and ^{10}Be in the northeastern Pacific Ocean, *Geochim. Cosmochim. Acta, 57*, 205-217, 1993.

Leynaert, A., D.M. Nelson, B. Quéguiner, and P. Tréguer, The silica cycle in the Antarctic ocean: is the Weddell sea atypical?, *Mar. Ecol. Prog. Ser., 96*, 1-15, 1993.

Mackensen, A., H. Grobe, H.-W. Hubberten, and G. Kuhn, Benthic foraminiferal assemblages and the δ^{13}C signal in the Atlantic sector of the Southern Ocean: Glacial to interglacial contrasts, in *Carbon Cycling in the Glacial Ocean: Constraints on the Ocean's Role in Global Change, NATO ASI Ser. I*, vol. 17, edited by R. Zahn et al., pp. 105-144, 1994.

Mangini, A., M. Jung, and S. Laukenmann, What do we learn from peaks of uranium and of manganese in deep sea sediments?, *Mar. Geol.*, in press, 2000.

Martin, J.H., Glacial-Interglacial CO_2 change: The iron hypothesis, *Paleoceanography, 5*, 1-13, 1990.

Martin, J.H., et al., Testing the iron hypothesis in ecosystems of the equatorial Pacific Ocean, *Nature, 371*, 123-129, 1994.

Martinson, D.G., N.G. Pisias, J.D. Hays, J. Imbrie, T.C. Moore Jr, and N.J. Shackleton, Age dating and the orbital theory of the ice ages: Development of a high-resolution 0 to 300,000 year chronostratigraphy, *Quat. Res., 27*, 1-29, 1987.

McManus, J., et al., Geochemistry of barium in marine sediments: Implications for its use as a paleoproxy, *Geochim. Cosmochim. Acta, 62*, 3453-3473, 1998.

McManus, J., W. M. Berelson, D. E. Hammond, and G. P. Klinkhammer, Barium cycling in the North Pacific: Implications for the utility of Ba as a paleoproductivity and paleoalkalinity proxy, *Paleoceanography, 14*, 53-61, 1999

Monaghan, M., S. Krishnaswami, and K.K. Turekian, The global average production rate of ^{10}Be, *Earth Planet. Sci. Lett., 76*, 279-287, 1985/86.

Monnin, C., C. Jeandel, T. Cattaldo, and F. Dehairs, The marine barite saturation state of the world's oceans, *Mar. Chem., 65*, 253-261, 1999.

Moore, J.K., M.R. Abbott, J.R. Richman, and D.M. Nelson, The Southern Ocean at the Last Glacial Maximum: A strong sink for atmospheric carbon dioxide, *Global Biogeochem. Cycles, 14*, 455-475, 2000.

Mortlock, R.A., C.D. Charles, P.N. Froelich, M.A. Zibello, J. Saltzman, J.D. Hays, and L.H. Burckle, Evidence for lower productivity in the Antarctic Ocean during the last glaciation, *Nature, 351*, 220-223, 1991.

Nelson, D.M., P. Tréguer, M.A. Brzezinski, A. Leynaert, and B. Quéguiner, Production and dissolution of biogenic silica in the ocean: Revised global estimates, comparison with regional data and relationship to biogenic sedimentation, *Global Biogeochem. Cycles, 9*, 359-372, 1995.

Niebler, H.-S., Reconstruction of plaeo-environmental parameters using stable isotopes and faunal assemblages of planktonic foraminifera in the South Atlantic Ocean, *Ber. Polarforsch., 167*, 198 pp., 1995.

Nürnberg, C.C., G. Bohrmann, M. Schlüter, and M. Frank, Barium accumulation in the Atlantic sector of the Southern Ocean: Results from 190,000 year records, *Paleoceanography, 12*, 594-603, 1997.

Peterson, R.G., and L. Stramma, Upper-level circulation in the South Atlantic Ocean, *Prog. Oceanogr., 26*, 1-73, 1991.

Petit, J.R., L. Mounier, J. Jouzel, Y.S. Korotkevich, V.I. Kotlyakov, and C. Lorius, Paleoclimatological and chronological implications of the Vostok core dust record, *Nature, 343*, 56-58, 1990.

Petschick, R., G. Kuhn, and F.X. Gingele, Clay mineral distribution in surface sediments of the South Atlantic: sources transport and relation to oceanography, *Mar. Geol., 130*, 203-229, 1996

Pichon, J.J., G. Bareille, M. Labracherie, L.D. Labeyrie, A. Baudrimont, and J.L. Touron, Quantification of the biogenic silica dissolution in Southern Ocean sediments, *Quat. Res., 37*, 361-378, 1992.

Pondaven, P., O. Ragueneau, P. Tréguer, A. Hauvespre, L. Dezileau, and J.L. Reyss, Resolving the "opal paradox" in the Southern Ocean, *Nature, 405*, 168-172, 2000.

Rosenthal, Y., E.A. Boyle, L. Labeyrie, and D. Oppo, Glacial enrichments of authigenic Cd and U in Subantarctic sediments: A climatic control on the elements' oceanic budget?, *Paleoceanography, 10*, 395-413, 1995a.

Rosenthal, Y., P. Lam, E.A. Boyle, and J. Thomson, Authigenic cadmium enrichment in suboxic sediments: Precipitation and postdepositional mobility, *Earth Planet. Sci. Lett., 132*, 99-111, 1995b.

Rutgers van der Loeff, M.M., and M. Hoppema, Shallow mineralization in the Weddell Gyre II: Evidence from ^{234}Th and TCO_2 budgets, *Eos Trans. AGU, 80*, (49), 103, 1999.

Rutgers van der Loeff, M.M., and G.W. Berger, Scavenging and particle flux: Seasonal and regional variations in the Southern Ocean (Atlantic sector), *Mar. Chem, 35*, 553-567, 1991.

Rutgers van der Loeff, M.M., and G.W. Berger, Scavenging of ^{230}Th and ^{231}Pa near the Antarctic Polar Front in the South Atlantic, *Deep Sea Res., Part I, 40*, 339-357, 1993.

Sarmiento, J.L., and R.A. Toggweiler, A new model for the role of the oceans in determining atmospheric pCO_2, *Nature, 308*, 621-624, 1984.

Schlüter, M., Organic carbon flux and oxygen penetration into sediments of the Weddell Sea: Indicators for regional differences in export production, *Mar. Chem., 35*, 569-579, 1991.

Schlüter, M., M.M. Rutgers van der Loeff, O. Holby, and G. Kuhn, Silica cycle in surface sediments of the South Atlantic, *Deep Sea Res., Part I, 45*, 1085-1109, 1998.

Sharma, P., P. Mahannah, W.S. Moore, T.L. Ku, J.R. Southon, Transport of ^{10}Be and ^{9}Be in the ocean, *Earth Planet. Sci. Lett. 86*, 69-76, 1987.

Shemesh, A., S.A. Macko, C.D. Charles, and G.H. Rau, Isotopic evidence for reduced productivity in the glacial Southern Ocean, *Science, 262*, 407-410.

Shimmield, G., S. Derrick, A. Mackensen, H. Grobe, and C. Pudsey, The history of barium, biogenic silica and organic carbon accumulation in the Weddell Sea and Antarctic Ocean over the last 150,000 years, in *Carbon Cycling in the Glacial Ocean: Constraints on the Ocean's Role in Global Change, NATO ASI Ser. I*, vol. 17, edited by R. Zahn et al., pp. 555-574, 1994.

Siegenthaler, U., and T. Wenk, Rapid atmospheric CO_2 variations and ocean circulation, *Nature, 308*, 624-626, 1984.

Singer, A., and A. Shemesh, Climatically linked carbon isotope variation during the past 430000 years in Southern Ocean sediments, *Paleoceanography, 10*, 171-177, 1995.

Smetacek, V., R. Scharek, L.I. Gordon, H. Eicken, E. Fahrbach, G. Rohardt, and S. Moore, Early spring phytoplankton blooms in ice platelet layers of the southern Weddell Sea, Antarctica, *Deep Sea Res., 39*, 153-168, 1992.

Spencer, D.W., M.P. Bacon, and P.J. Brewer, Models of the distribution of ^{210}Pb in a section across the north equatorial Atlantic Ocean, *J. Mar. Res., 39*, 119-138, 1981.

Stephens, B.B., and R.F. Keeling, The influence of Antarctic sea ice on glacial-interglacial CO2 variations, *Nature, 404*, 171-174, 2000.

Thomson, J., N.C. Higgs, T.R.S. Wilson, I.W. Croudace, G.J. deLange, and P.J.M. vanSandfoort, Redistribution and geochemical behaviour of redox-sensitive elements around S1, the most recent eastern Mediterranean sapropel, *Geochim. Cosmochim. Acta, 59*, 3487-3502, 1995.

Usbeck, R., Modelling of marine biogeochemical cycles with an emphasis on vertical particle flux, *Ber. Polarforsch., 332*, 105 p., 1999.

Usbeck, R., and R. Schlitzer, Shallow remineralization in the Weddell Gyre I: Particle fluxes from inverse modeling, *Eos Trans. AGU, 80*, (49), 191, 1999.

Walter, H.J., M.M. Rutgers van der Loeff, and H. Hoeltzen, Enhanced scavenging of ^{231}Pa relative to ^{230}Th in the South Atlantic south of the Polar Front: Implications for the use of the ^{231}Pa/^{230}Th ratio as a paleoproductivity proxy, *Earth Planet. Sci. Lett., 149*, 85-100, 1997.

Walter, H.J., M.M. Rutgers van der Loeff, and R. Francois, Reliability of the ^{231}Pa/^{230}Th activity ratio as a tracer for bioproductivity of the ocean, in *Use of Proxies in Paleoceanography: Examples from the South Atlantic*, edited by G. Fischer and G. Wefer, pp. 393-408, Springer-Verlag, New York, 1999.

Walter, H.J., M.M. Rutgers van der Loeff, and H. Hoeltzen, and U. Bathmann, Reduced scavenging of ^{230}Th in the Weddell Sea: Implications for paleoceanographic reconstructions in the South Atlantic, *Deep Sea Res., Part I, 47*, 1369-1387, 2000.

Wang, L., T.L. Ku, S. Luo, J.R. Southon, and M. Kusakabe, ^{26}Al-^{10}Be systematics in deep-sea sediments, *Geochim. Cosmochim. Acta, 60*, 109-119, 1997.

Wedepohl, K.H., The composition of the continental crust, *Geochim. Cosmochim. Acta, 59*, 1217-1232, 1995.

Wefer, G., and G. Fischer, Annual primary production and export flux in the Southern Ocean from sediment trap data, *Mar. Chem., 35*, 597-613, 1991.

Yu, E.F., Variations in the particulate flux of ^{230}Th and ^{231}Pa and paleoceanographic applications of the ^{231}Pa/^{230}Th ratio, Ph.D. thesis, 269 pp., Woods Hole Oceanogr. Inst., Woods Hole, Mass., 1994.

Yu, E.F., R. Francois, and M.P. Bacon, Similar rates of modern and last-glacial ocean thermohaline circulation inferred from radiochemical data, *Nature, 379*, 689-694, 1996.

Zielinski, U., and R. Gersonde, Diatom distribution in Southern Ocean surface sediments (Atlantic sector): Implications for paleoenvironmental reconstructions, *Palaeogeogr. Palaeoclimatol. Palaeoecol., 129*, 213-250, 1997.

Zielinski, U., R. Gersonde, R. Sieger, and D. Fütterer, Quaternary surface water temperature estimations; calibration of a diatom transfer function for the Southern Ocean, *Paleoceanography, 13*, 365-383, 1998.

G. Bohrmann and C.C. Nürnberg, GEOMAR, Forschungszentrum für marine Geowissenschaften, Wischhofstrasse 1-3, 24148 Kiel, Germany. (gbohrmann@geomar.de; dnuernberg@geomar.de.)

M. Frank, Institute for Isotope Geology and Mineral Resources, Department of Earth Sciences, ETH Zentrum, NO C61, Sonneggstrasse 5, CH-8092 Zürich, Switzerland. (frank@erdw.ethz.ch.)

A. Mangini, Heidelberger Akademie der Wissenschaften, c/o Institut für Umweltphysik, Universität Heidelberg, Heidelberg, Germany. (Augusto.Mangini@iup.uni-heidelberg.de)

R. Gersonde and M.M. Rutgers van der Loeff, Alfred-Wegener-Institut für Polar- und Meeresforschung, Columbusstrasse, 27568 Bremerhaven, Germany. (RGersonde@AWI-Bremerhaven.de; Loeff@AWI-Bremerhaven.de)

P.W. Kubik, Paul Scherrer Institut, c/o Institut für Teilchenphysik der ETH Zürich, ETH-Hönggerberg, CH-8093, Zürich, Switzerland. (Kubik@particle.phys.ethz.ch)

M. Suter, Institut für Teilchenphysik der ETH Zürich, ETH-Hönggerberg, CH-8093 Zürich, Switzerland. (Martin.Suter@particle.phys.ethz.ch)

(Received January 3, 2000;
revised June 27, 2000;
accepted July 25, 2000.)